CZECH TECHNICAL UNIVERSITY IN PRAGUE

FACULTY OF MECHANICAL ENGINEERING
DEPARTMENT OF PROCESS ENGINEERING

EXPERIMENTAL TESTING OF CO2 SEPARATION FROM FLUE GAS BY GAS MEMBRANE PROCESSES

MASTER'S THESIS

2021 DANIEL JAKUB HRTUS

ZADÁNÍ DIPLOMOVÉ PRÁCE

I. OSOBNÍ A STUDIJNÍ ÚDAJE

Příjmení: **Hrtus** Jméno: **Daniel Jakub** Osobní číslo: **437079**

Fakulta/ústav: **Fakulta strojní**

Zadávající katedra/ústav: **Ústav procesní a zpracovatelské techniky**

Studijní program: **Strojní inženýrství**

Studijní obor: **Procesní technika**

II. ÚDAJE K DIPLOMOVÉ PRÁCI

Název diplomové práce:

Experimentální testování polymerních membrán pro separaci CO2 z emisních plynů.

Název diplomové práce anglicky:

Experimental testing of CO2 separation from flue gas by gas membrane processes

Pokyny pro vypracování:

Zpracujte teoretickou rešerši zaměřenou na možnosti využití membráno-vých procesů pro separaci CO2 z emisních plynů. Na laboratorní jednotce otestujte účinnost separace CO2 z modelových spalin v závislosti na charakteristice membránového modulu a procesních podmínkách.

Seznam doporučené literatury:

Dle doporučení vedoucího práce.

Jméno a pracoviště vedoucí(ho) diplomové práce:

doc. Ing. Lukáš Krátký, Ph.D., ústav procesní a zpracovatelské techniky FS

Jméno a pracoviště druhé(ho) vedoucí(ho) nebo konzultanta(ky) diplomové práce:

Datum zadání diplomové práce: **21.04.2021** Termín odevzdání diplomové práce: **13.08.2021**

Platnost zadání diplomové práce: **19.09.2021**

doc. Ing. Lukáš Krátký, Ph.D. podpis vedoucí(ho) práce	prof. Ing. Tomáš Jirout, Ph.D. podpis vedoucí(ho) ústavu/katedry	prof. Ing. Michael Valášek, DrSc. podpis děkana(ky)

III. PŘEVZETÍ ZADÁNÍ

Diplomant bere na vědomí, že je povinen vypracovat diplomovou práci samostatně, bez cizí pomoci, s výjimkou poskytnutých konzultací. Seznam použité literatury, jiných pramenů a jmen konzultantů je třeba uvést v diplomové práci.

Datum převzetí zadání Podpis studenta

Affidavit

I hereby confirm that the master's thesis was written independently under the guidance of my supervisor – Assoc. Prof. Ing. Lukáš Krátký, Ph.D. I exclusively used the cited literature referenced at the end.

Prehlasujem, že som túto prácu vypracoval samostatne a pod vedením doc. Ing. Lukáša Krátkého, Ph.D. Použil som výhradne pramene a literatúru uvedenú v zozname zdrojov na konci práce.

In Prague…… …….

Daniel Hrtus

First and foremost, I would like to thank my supervisor Assoc. prof. Ing. Lukáš Krátky, Ph.D for his patience and his insights. Additionally, I would like to thank my family for all the support throughout my lengthy studies.

Annotation sheet

Name: Daniel Jakub
Surname: Hrtus
Titul: Experimentální testování polymerních membrán pro separaci CO2 z emisních plynů
Title: Experimental testing of CO2 separation from flue gas by gas membrane processes
Scope of work: number of pages: 62
number of figures: 33
number of tables: 13
Academic year: 2020/2021
Language: English
Department: Department of Process Engineering
Study program: N2301 Mechanical Engineering
Specialization: 3909T012 Process Engineering
Supervisor: Assoc. prof. Ing. Lukáš Krátky, Ph.D

Key words: barrer, carbon dioxide, emission, feed, GPU, hollow fiber, permeate, polymer, retentate, selectivity, recovery

Kľúčové slová: barrer, oxid uhličitý, emisia, feed, GPU, duté vlákno, permeát, polymer, retentát, selektivita, recovery

Annotation: This diploma thesis focuses on membrane gas separation, more specifically carbon dioxide membrane separation from flue gas. The work has a research part describing gas membrane separation principles, and an experimental part that describes gas membrane separation using hollow fiber module and a description of separation process parameters.

Anotácia: Táto diplomová práca sa zameriava na membránovú separáciu plynov, presnejšie na separáciu oxidu uhličitého zo spalín. Práca má rešeršnú časť, v ktorej sú opísané princípy membránovej separácie plynov a experimentálnu časť, ktorá sa venuje separácii plynov na module s dutými vláknami a neskôr opisu procesných parametrov separácie.

Contents

Nomenclature

A	area [m^2]
c	concentration [% volumetric]
d	diameter [m]
J	molar flux [mol s^{-1} m^{-2}]
l	thickness [mm]
$\dot{m}$	mass flowrate [g/h] [g/s]
M	molecular mass [g mol^{-1}]
$\dot{n}$	molar flowrate [mol s^{-1}]
P	permeability [barrer]
p	pressure [bar] [MPa]
R	universal gas constant [J K^{-1} mol^{-1}]
S	separation coefficient
T	temperature [°C] [K]
x	molar fraction
y	molar fraction

Greek

α	selectivity
η	recovery
θ	permeation number
ϕ	pressure ratio
Π	permeance [GPU]

Indices

A, B, I	gas species
F	feed
g	glass
K	Knudsen
m	melt
P	Poiseuille
P	permeate
p	pore

1.Introduction – CO_2 as greenhouse gas

The role of atmosphere as a de-facto Earth's thermostat has been closely studied since the early nineteenth century. Big-name scientists like Fourier of Arrhenius who studied this phenomenon also recognized carbon dioxide's role in the absorption of thermal wavelengths from solar radiation. In short, greenhouse gases (GHGs) absorb heat that would otherwise get reflected back to space and therefore cause a raise of temperature in the lower atmosphere.[1] Although the greenhouse effect (GHE) had been studied for some time, the effect of human activities on it was not considered much until 1970s and since then, the emissions have more than doubled, as seen in Figure 1.[2]

The greenhouse effect is an important mechanism that allows life on earth thrive, quantitatively its overall effect is 33°C. CO_2 is by itself responsible for 7°C but, when enhanced by the most abundant GHG that is H_2O, its effect is tripled. The current atmospheric CO_2 concentration of over 400 ppm is the highest to date and it is going up by 2 ppm every year.[1] This means that the study of its potential negative effects and warnings about the impact of human activity on the GHE are well based.

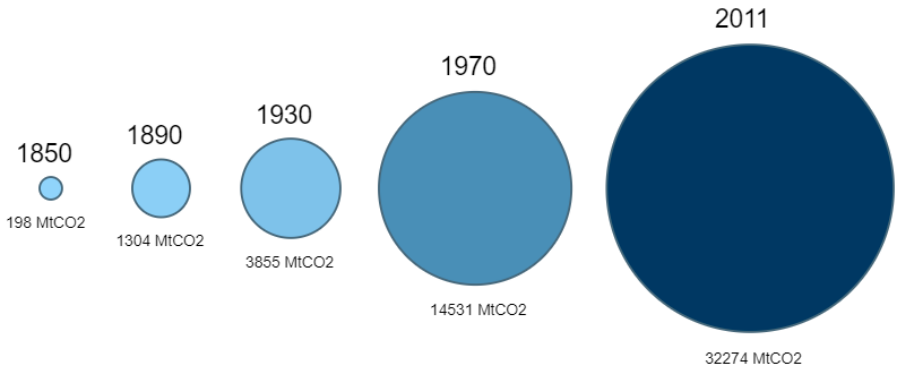

Figure 1. Worldwide emissions in megatons of carbon dioxide since the end of the industrial revolution. In a century and a half we saw a 160-fold increase in CO_2 emissions.[2]

The risks tied to the GHE amplification are serious and include increase in heat-related mortality, severe droughts and water shortages, damages from wildfires, river and coastal floods, reduced catch potential and food production as well as food quality, loss of ecosystems and more.[3]

Although all these changes would take effect globally, the CO_2 producers are distributed unevenly among nations – with USA leading the overall CO_2 emissions historically until 2006 when it got overtaken by China, the leading emitter nowadays. India, as another prospering economy, places third, followed by Russia, Japan, and the United Kingdom. Regionally though, the north American area tops the chart of per capita emissions at almost 17 t of CO_2, while the European and central Asian regions combined stand at 7.3 t of CO_2 (in 2018).[2]

Considering the mounting evidence, governments all around the world have been changing policies and setting targets to reduce CO_2 emissions and mitigate the GHE ramp up. The formal goal being to keep the global temperature raise below 2°C at worst – as per the Paris Agreement.[4] Unfortunately the solutions do not come easy as the socio-economic factors that are tied to CO_2 emissions can be quite varied and include the income growth of a country, effect of agricultural production and use of fertilizers, tourism, trade openness and more.[5]

The focus of this work is two-fold – first we aim to familiarize the reader with the relatively novel approach to CO_2 emission mitigation by using membrane separation. The first -theoretical - part analyzes how CO_2 is emitted by the industry sector via flue gas emissions. Then, we list competing technologies and analyze how they stack up against membrane separation and at the end of the theoretical section, we discuss the existing membrane technology nowadays. Second, we present the experimental work done on our gas membrane separation unit. We focused on an area that is still yet to be researched in depth and that is the effect of flue gas composition on membrane CO_2 separation.

2. CO_2 separation nowadays

2.1. CO_2 emissions by the industry sector

In context of our work that discusses technological solutions to the GHE problem we were mostly interested in emissions by the industry sector. From a Sankey diagram in **Figure 2** we see that at around 30% of total GHG emissions, the industry sector is a major contributor (the width of a line represents the amount of GHG emissions so the wider the line the more emissions produced by said entity).[6]

When broken down, CO_2 emissions from the industry sector come from production of cement, steel, and iron (44%) while the rest comes from chemicals and fertilizers production, paper and pulp processing aluminum production and food processing.[6,7] For example, the cement industry itself accounts for around 6% of global CO_2 emissions and to produce 1 ton of cement 900 kg of carbon dioxide is released.[8] Approximately 98% of direct CO_2 emissions in the industry sector are being released by manufacturing of products. This means they are a consequence of either chemical reactions or burning of fossil fuels that provides the heat necessary for these reactions. In 2010 the amount of worldwide process CO_2 emissions was 2.59 $GtCO_2$ eq, while in 1990 it was roughly half the amount.[6]

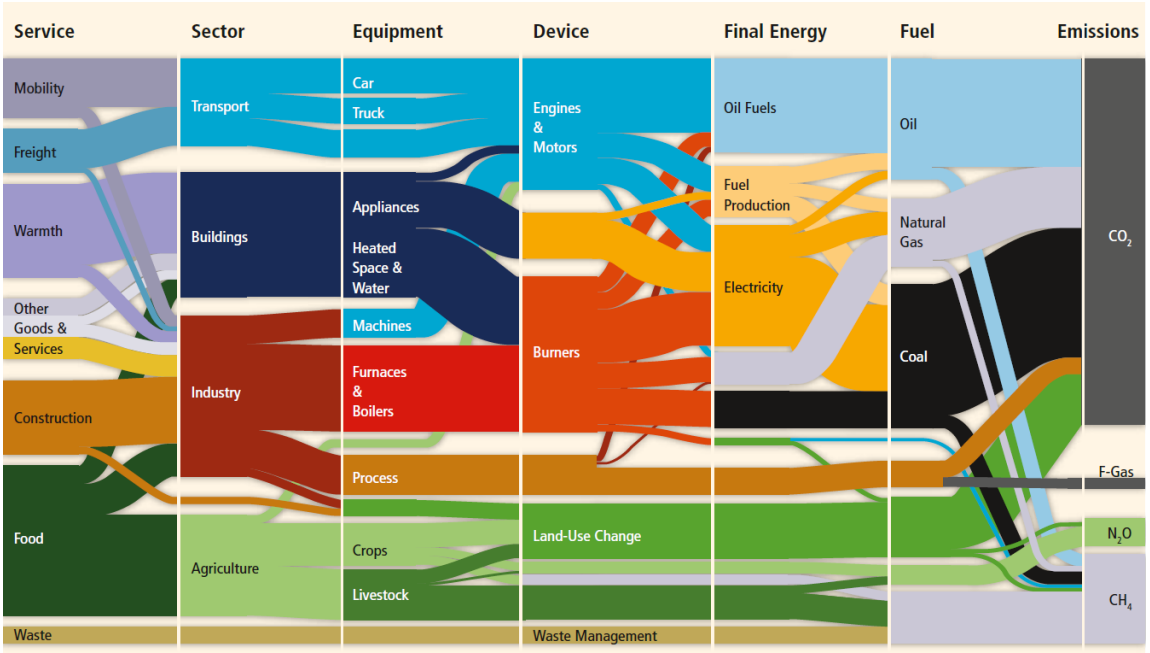

Figure 2. A system breakdown of GHG emissions via a Sankey diagram. It shows how demand for services is turned into emissions – a sum of line widths for any cross section equals the total amount of emissions and is

constant throughout the diagram. Industry sector is a major contributor with furnaces and boilers being among the most used equipment.[6]

2.1.1. Emission composition

For efficient separation, it is crucial to know the exact composition of the stream although, especially for research purposes, the focus is usually on the major stream component. CO_2 separation from streams has been in practice for a long time and in industrial scenarios it is present with either H_2, CH_4 or N_2.[9] Therefore, whenever we talk about separation in this work, we will note it as CO_2/ XXX meaning separation of CO_2 from a stream that mainly contains gas XXX while recognizing that there are usually more compounds present in the stream (as seen in Table 1).

CO_2/H_2 separation is required mostly in the process of H_2 production and CO_2/CH_4 separation is used in natural gas purification. In both cases, the goal is to obtain a cleaner gas of value. In case of CO_2/N_2 separation on the other hand, the goal is to get rid of CO_2 not for the value of N_2 but for the negative effects of CO_2 itself. This is also the case for us, as CO_2/N_2 separation is needed for flue gas streams that generally contain about 80% of N_2 and 5-20% of CO_2 (in coal-fired power plants the more accurate estimate is 13-15% of CO_2).[9,10] Of course, the flue gas composition depends on the fuel type and quality, Table 2 offers exact flue gas composition for low sulfur coal.[11]

Table 1. Emission streams and their composition. The bulk of separation efforts is focused on CO_2/N_2 separation as this gas composition comes from burning of fossil fuels[9]

	Source process	Separation	Gas composition	Process conditions
Flue gas streams	Power plants Coal gasification plants Steel factory Cement factory Transportation	CO_2/N_2	5-25% CO_2 65-80% N_2 3-5% O_2 Rest: N2, SO_x, H_2S, H_2O	35-100 °C 1 bar
Natural gas	Natural gas pipes Sweetening of natural gas	CO_2/CH_4	1-8% CO_2 70-90% CH_4 0-20% C_2H_6, C_3H_8, C_4H_{10} Rest: O_2, N_2, H_2S, Ar, Xe, He	25-30 °C 1.2 bar
Biogas	Various		34-40% CO_2 50-70% CH_4 Rest: N_2, O_2, H_2S, H_2O	25-35 °C 1 bar

Table 2. Flue gas composition components (excluding nitrogen) from low sulfur coal.[12]

Component	Concentration
H_2O	5-7%
O_2	3-4%
CO_2	15-16%
Hg complexes	1 ppb
CO	20 ppm
Hydrocarbons	10 ppm
HCl	100 ppm
SO_2	800 ppm
SO_3	10 ppm
NO_x	500 ppm

2.2. CCS and CO_2 separation methods

Carbon capture and storage (CCS) is the main proposed long-term solution the problem of reducing CO2 emissions (the most viable short-term solution seems to be improving process efficiencies).[13] The idea of CCS is to separate CO2 from given industrial process – be it power plants, cement plants, steel-production plants, etc. - and store it in porous geological formations or empty oil/gas reservoirs (more than 800 such formations have been identified all over the world).[14,4,9]

There are 3 main options to capturing CO2: (i) pre-combustion capture, (ii) oxy-fuel combustion and (iii) post-combustion capture. The pre-combustion capture, formally known as integrated gasification combined cycle (IGCC-CCS), is based on reaction of fuel and O2 (air) or steam to produce what is called syngas. Syngas is composed primarily of carbon monoxide and hydrogen and is subsequently shifted, and CO2 is then separated from product gas. Oxy-fuel combustion involves burning fuel in the presence of oxygen and recycled CO2, which leads to a stream of CO2 and H2O and their subsequent separation by condensation. The post-combustion capture uses separation processes to remove CO2 from the flue gas.[13] Membrane separation is meant to be used in the post-combustion capture.

CO2 and its rather complicated phase diagram, as seen in Figure 3, poses a challenge for capturing and separation. It is usually stored in large volumes and as such, the requirement for it is to have low density which is the case in its supercritical phase (that means high pressure and thus high compression cost). [9]

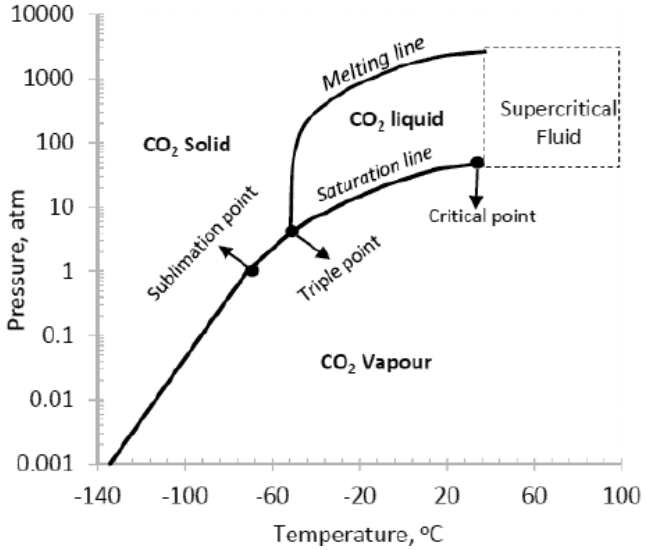

Figure 3. CO_2 phase diagram. For high-volume storage, CO_2 must be in supercritical condition requiring high pressure and resulting in increased cost.[9]

Notable methods for CO_2 separation include: (i) absorption, (ii) adsorption and (iii) for the more traditional ones while the latest technology added to the list is (iv) membrane separation.[4,9]

CO_2 absorption

Absorption refers to separation of CO_2 from a mixture using a liquid absorbent and the process itself has either chemical (gas reacts with the absorbent) or a physical (gas is dissolved in absorbent based on Henry's law) character.[4] In an absorption column, CO2 is absorbed into the absorbent solution (these are amine-based), then stripped from it and later compressed for transportation.[14] A big challenge this method is facing is the degradation of amine solvents into toxic compounds that damage the equipment, and ultimately this degradation leads to sorbent loss.[9]

CO_2 adsorption

This method refers to uptake of CO_2 gas by a selective solid porous sorbent. This is done in a solid bed adsorber column. The release of captured CO2 is done by changing process parameters – e.g., decreasing column pressure or increasing temperature. There are 2 types of adsorptions and that is physical – based on van der Waals force – and chemical – based on chemical bonding. For physical sorption, zeolite and activated carbon materials are commonly used and a big advantage of this technology is that the materials can be adsorbed/desorbed in repeated cycles. For chemical adsorption calcium oxides, lithium silicate and amine-supported porous materials are used. Chemical adsorption allows for use in higher temperatures but lacks in the regenerative capability. [13,4] Main properties of the sorbent material then include its surface area, selectivity and regenerability.[9]

CO_2 cryogenic distillation

Distillation in general is based on different boiling points of mixture compounds. Cryogenic distillation works at very low temperatures (approx. -110°C) and high pressures. Under such conditions, CO2 is solidified and removed from the rest of gases. It is a well-known but highly energy-intensive process.[9]

CO_2 membrane separation

The driving force in membrane separation is the pressure and/or concentration gradient. Membrane materials are designed in such way that they allow for passing of selected gas from given mixture.[9] The interaction between gases and membrane materials, much like in previous

cases, can be physical or chemical.[15] We will cover membrane separation in more detail in the following chapters.

Table 3 offers a brief comparison between the separation processes we mentioned. Absorption is the most widespread technology in relation to CO2 separation, however membrane separation seems to be leading charge in terms of potential industrial use, but more research is needed to fully weigh its benefits.

Table 3 Separation methods used in CO2 separation and their comparison. Absorption using amines is the most prevalent technology in this field nowadays. Membrane separation, on the other hand, is the most recent technology and has its benefits, though more research is needed.[9]

Technology	**Advantage**	**Disadvantage**
Absorption	→ High absorption efficiency (>90%) → Sorbents can be regenerated by heating and/or depressurization → Most mature process for CO2 separation	→ Absorption efficiency depends on CO2 concentration → Significant amounts of heat for absorbent regeneration are required → Environmental impacts related to sorbent degradation
Adsorption	→ Reversible process and recyclable adsorbent → High adsorption efficiency (>85%)	→ Requires high temperature adsorbent → High energy required for CO2 desorption
Cryogenic distillation	→ Mature technology → Adopted for many years in CO2 recovery industry	→ Viable only for very high CO2 concentration (>90% vol.) → Requires low temperatures and thus is quite energetically demanding
Membrane separation	→ High separation efficiency can be achieved (>80%) → Operation and equipment simplicity → No phase change → Process is flexible and can be adopted for separation of various gases	→ Operational problems like low fluxes and fouling need to be addressed → More research on scale-up required

A projection done by the U.S. Department of Energy showed a 30-40% increase in electricity price would occur with massive deployment of post-combustion capture using amine solvents. What is more, flue gas containing CO_2 and leaving power plants and most industrial processes where fossil fuels are burned, offers no profit margin for treatment. This means that a separation cost of around 25 USD/ton would further raise the cost of the whole operation while incurring additional increase in electricity price.[9] This alone has been a major motivation in exploring

solutions that would offer process cost reduction while maintaining similar or better separation efficiencies. Membrane separation – which we explore in upcoming paragraphs - is a good candidate for replacing the traditional separation methods.

3.Membrane separation of gases

Membrane separation of gases has become a notable technological process during the last 25 years. The foundation was laid out in the 19th century by Thomas Graham who dedicated his research to study of gas transport through thin barriers and, as such, laid a foundation for a diffusion-solution gas transport model. The first commercial gas separation unit was introduced in 1980 by Monsato and it used PRISM™ modules and was used in H_2 separation for NH_3 production. Soon after, other companies followed and in mid 1980s membrane units for CO_2 separation from natural gas were being supplied.[16] Process parameters and membrane properties are a good metric of just far the technology has come. In the beginning of its industrial use, the volumetric flows we usually in tens of thousands of cubic meters per hour, while today the numbers are in hundreds to millions of m^3/h. Similarly, the membrane thicknesses used to be around 200 nm while today the number are in tens of nm.[17] What is more, the membrane business has grown significantly with the worldwide annual turnaround of gas membrane technology market in 2015 being 1695 millions of USD (which was a 50% growth since 2010).[16] Membranes have a potential to completely replace the traditional separation methods or they may be deployed in conjunction with them. Membrane acid gas separation systems fall into these categories: (1) miniature setups with capacities < $140x10^3$ m^3/d, where membrane systems are feasible and appealing; (2) small setups ($140x10^3$ – $1133x10^3$ m^3/d), where amine-based separation and membrane separation compete, and the preference is case-specific; (3) medium to big setups (capacities > $1133x10^3$ $m3/d$), where it is not feasible to use membranes over amine-based absorption.[18]

The advantages gas membrane separation brings are plenty (Table 3). The most notable ones are the possibility of lower temperature separation, lack of necessary additives and operation and capital cost savings.[4,16] In our case – post combustion flue gas CO_2 separation as seen in **Figure 4** – more than 50% of the operation cost lies in powering the vacuum pump on the permeate side. The capital costs (membrane module and piping) are high as the membrane area needs to be large because of low pressure difference.[4]

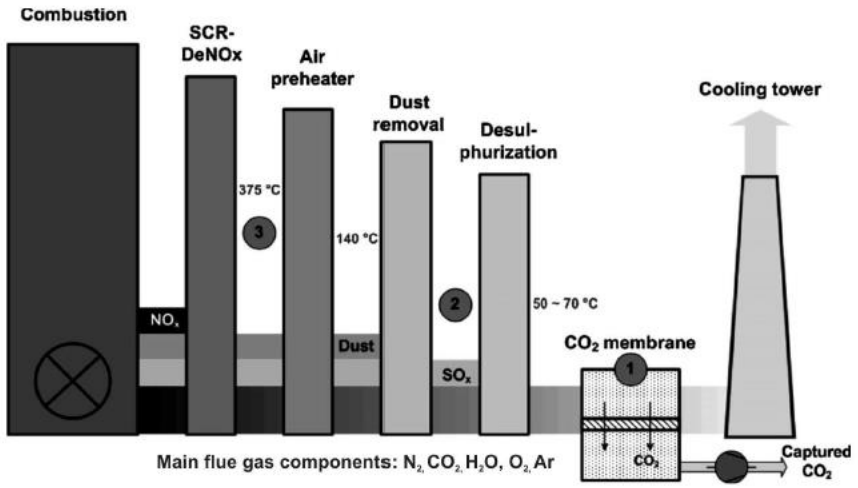

Figure 4. CO2 membrane separation in post-combustion separation from flue gas.[9]

3.1. Gas membrane separation terminology

When reading about a specific technical are such as gas membrane separation, it is always useful to establish the argot and so what follows are the most useful technical terms needed to understand this work.

Permeate and retentate: Feed stream is divided on the membrane interface into two streams – the one that stays on the same side of the membrane is called retentate while the stream richer in gas we want to separate is called permeate. This principle is displayed clearly in **Figure 5**.

Permeation of gas: Division of gaseous mixture using a porous polymeric membrane that allows for selective passing of given component. The driving force of membrane separation is pressure gradient. [15] It is one of two main membrane parameters by which the performance is judged, as seen in **Figure 6**.

Selectivity: Membrane characteristic that quantifies passing of given gas mixture component over another one (put simply, selectivity shows membranes "preference" towards given gas). The metric by which permeability is shown is the fraction of gases *A* and *B* - $\alpha_{A/B}$.[9,15] It is the second main membrane characteristic, as seen in **Figure 6**.

Separation efficiency (recovery): This quantity describes the rate of mass flow of separated component *A* in permeate - $\dot{m}_A^P$ - and the mass flow of the same component in feed - $\dot{m}_A^F$.

$$\eta_A = (\dot{m}_A^P / \dot{m}_A^F) \cdot 100 \qquad \text{(eq.1)}$$

Permeance: The ability of a material to allow passing of fluids. Along with selectivity, it is the main characteristic of membrane separation productivity. Permeance tells us how much gas

passes through given membrane surface during given time for given pressure difference. The universally recognized unit for permeance is GPU, where:

$$1\ GPU = \ 7.501x10^{12} m^3_{STP} m^{-2} s^{-1} Pa^{-1} \quad \text{(eq.2)}$$

$$1\ GPU = \ 3.35x10^{-10} mol\ m^{-2} s^{-1} Pa^{-1} \quad \text{(eq.3)}$$

The permeance is usually used when membrane's thickness is hard to determine, e.g., asymmetric membranes.[15,16]

Permeability: Material characteristic we get when permeance is multiplied by membrane's thickness. The permeability unit is Barrer[15]:

$$1\ Barrer = \ 3.35x10^{-16} mol\ m\ m^{-2} s^{-1} Pa^{-1} \quad \text{(eq.4)}$$

Graham's law: Says that a gas rate of diffusion is inversely proportional to its molecular weight. It can be written as:

$$\frac{v_A}{v_B} = \left(\frac{M_B}{M_A}\right)^{\frac{1}{2}} \quad \text{(eq.4)}$$

where v_A is the rate of diffusion of component *A* [$m^3.s^{-1}$] or [$mol.s^{-1}$], v_B is the rate of diffusion of gas component *B* [$m^3.s^{-1}$] or [$mol.s^{-1}$], M_A a M_B are molecular weights of gas *A* and gas *B* [$kg.mol^{-1}$].

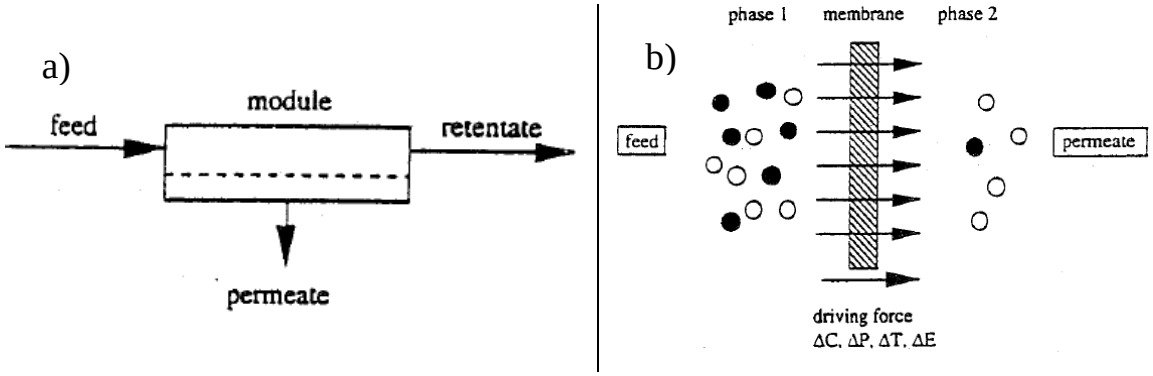

Figure 5. Principle of membrane separation: a) feed gas is divided into retentate and permeate streams; b) feed (phase 1) and permeate (phase 2) are separated by the membrane interface , the driving force of this separation is mainly pressure difference between the 2 phases.[19]

Fick's first law: Relates the concentration to the diffusion flux by stating that flux occurs in the direction from higher to lower concentrations (proportionally to the concentration gradient).[15]

Fick's second law: Describes diffusion change in time.

Henry's law: states that at constant temperature, the amount of gas dissolved in liquid of given volume is proportional to the partial pressure of said gas (p_A) in equilibrium with that liquid.

$$p_A = H * x_A \quad \text{(eq.5)}$$

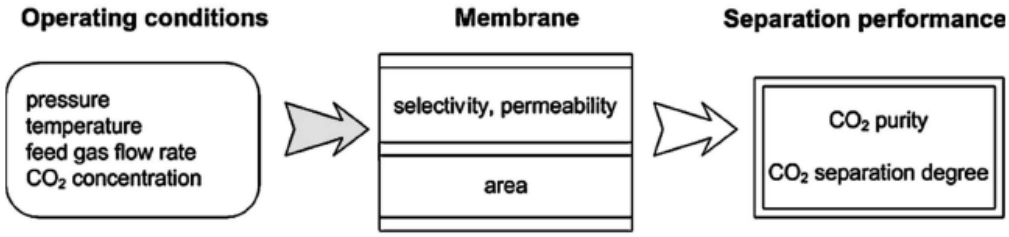

Figure 6. Chain of parameters that influence membrane separation. Good separation degree is achieved by proper membrane material and module selection. Membrane parameters are, in turn, selected based on the operating conditions and gas feed gas properties.[9]

Pore: A small opening in membrane structure. **Table 4** shows the classification of pore sizes. A commonly used unit in membrane science for describing pore sizes or molecule sizes is *Å* (angstrom), where *1 Å = 0.1 nm.*

Mean free path: The molecules of gas passing through a membrane not only hit the pore walls but also each other. Mean free path is defined as the average distance a molecule travels without colliding with another molecule. This path is referenced to the molecule's size – the bigger the molecule, the shorter its mean free path.[15] For component *i* it is defined by following equation:

$$\lambda_i = (3\eta/2p)(\sqrt{\pi RT}/2M) \quad \text{(eq.6)}$$

where η is the gas viscosity, R is the universal gas constant, T is the temperature, M is the molecular weight, and p is the gas pressure.

Table 4. Classification of pore diameter sizes according to the IUPAC (International Union of Pure and Applied Chemistry).[15]

<table>
<tr><th colspan="2">Micropores</th><th>Mesopores</th><th>Macropores</th></tr>
<tr><td colspan="2">d_p < 2 nm</td><td rowspan="3">2-50 nm</td><td rowspan="3">d_p > 50 nm</td></tr>
<tr><td>Ultra-micropores</td><td>Super-micropores</td></tr>
<tr><td>d_p < 0.7 nm</td><td>d_p > 0.7 nm</td></tr>
</table>

Diffusion: Process by which gas molecules migrate from the zone of higher concentration to the zone of lower concentration. There are three types of diffusion: (i) Knudsen diffusion, (ii)

molecular diffusion (sieving) and (iii) surface diffusion. Additionally, in non-porous membranes, the separation happens via the diffusion-solution model. All these mechanisms are displayed in **Figure 7**.[9].

Knudsen diffusion: Occurs mostly in longer mesopores as the mean free path of gas molecules is significantly longer than the pore size. Under such conditions the molecules collide more frequently with the walls.[9]

Molecular diffusion: Occurs when the mean free path of gas molecules is shorter than the pore size and thus the molecules collide amongst each other more frequently. Driving force in this case is the concentration gradient. [9]

Surface diffusion: Happens when the separated gas compound has a strong affinity towards the membrane surface and therefore it is adsorbed on said surface. Surface diffusion usually occurs in conjunction with another diffusion type.[9]

Diffusion-solution: This transport mechanism occurs in non-porous/ dense membranes. Gas mixture passes through the membrane and certain components are separated based on different solubility – a component is separated by solution and diffusion into a dense material.[9]

Capillary condensation: At certain critical pressure the pores are filled with gas condensate and a liquid meniscus is formed at both pore openings. A hydrodynamic flow is induced by capillary pressure difference between these ends. Capillary condensation theoretically promotes high selectivity as the condensate blocks the pore for the non-condensing gas component.[9]

Molecular sieving: Happens in materials with very small holes with exact diameter. The pore diameter allows for smaller molecules to pass while stopping the bigger ones. Activated charcoal or silica gel are such materials.[15,9]

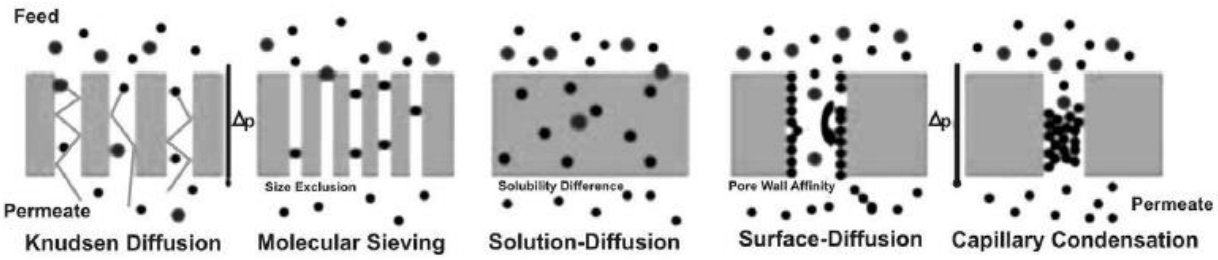

Figure 7. Different membrane gas separation principles.[9]

3.2. Membrane classification

Membrane properties are determined based on these criteria: (a) material (determines permeability and separation factor), (b) structure and membrane thickness (permeance), (c) membrane configuration and (d) membrane module. Membrane design must consider the main challenges, especially when the feed contains sulfur-based compounds such as H_2S or SO_2 that cause fouling – a buildup of solid matter on membrane pores. Fouling is usually reversible and is treated by heating the membrane up and flowing an inert gas through the pores. Compaction, which is tightening of pores caused by increased pressure is another complication that worsens separation capabilities and is usually irreversible. Other than these problems, there are others like different thermal expansions of certain module parts or simply big pressure drops.[15]

3.2.1. Membrane materials

Given the challenges we just listed, the properties we are looking for in membrane material are adequate mechanical and chemical durability, good permeability, and selectivity. Sorted by material, we know: (a) polymeric, (b) carbon, (c) ceramic and (d) metal membranes (a special category is so called membrane with facilitated transport (FTM) that contain a substance with a strong affinity to separated gas).[16] In regards to CO_2 separation from flue gas, we mainly talk about polymeric membranes but FTMs have been a target of research as well.[4] Next we are going to mention the basic theory of polymers.

Polymer is a material consisting of macromolecules that are further divided into smaller building blocks – monomers. Polymers are characterized by their high molecular weight. According to their molecular structure, polymers divided into: (i) linear, (ii) branched, (iii) cross-linked. This structure affects their physical and thermochemical properties.[9]

Polymers generally have 2 phases: (a) amorphous and (b) crystalline. it is rare for polymer to be in a fully crystalline form. The state of a polymer is given by its *glass transition temperature* T_g (for crystalline polymers, the guiding temperature is the *melting temperature* T_m) – see **Figure 8**. The macromolecular chains are organized sporadically in the amorphous phase and, when heated up beyond the glass transition point, they react, and the polymer state shifts from glassy to rubbery state. At T_m, lined-up chains are broken up into crystallites.

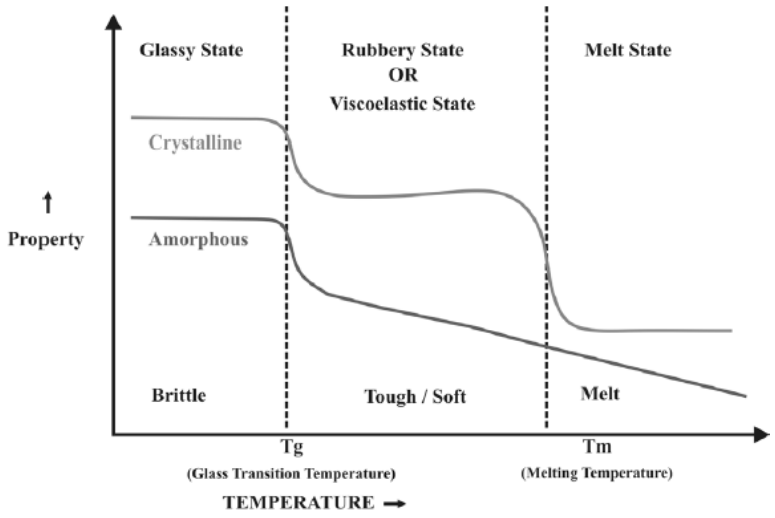

Figure 8. Polymer phases based on its temperature.[9]

The glassy state occurs at $T < T_g$ and glassy polymers are characteristic by being hard and brittle, a consequence of limited chain movement. Regarding the separation properties, the selectivity of glassy polymers is high, but gas diffusion is quite limited. In practice, they are preferred for their mechanical robustness and good selectivity (mainly based on molecular sieving). [9,16]

If $T > Tg$ and $T < T_m$ then the polymer is in its rubbery state, characterized by toughness and flexibility. Its selectivity in this state is a function of how much the gases condensate. Gas solubility in rubbery polymers follows Henry's law from eq.4. In commercial practice, silicone rubbers are used for steam separation from inert gases because of their good permeability and selectivity.[9,15]

3.2.2. Membrane modules

Industrial deployment of membranes requires big surface areas to be used to allow for efficient separation. Physical platforms in which membranes are housed, and which determine the membrane area, are called membrane modules. Gas feed entering the module is characterized by is flowrate, temperature, pressure, and composition. Crucial characteristics of membrane modules are its mechanical, thermal, and chemical durability, and an even stream distribution without formation of so-called dead zones. More characteristics include low pressure drop, cleaning ease, low manufacturing cost, and modularity. Most used membrane modules are: (a) planar, (b) spiral-wound, (c) tubular module, and (d) capillary and hollow-fiber module.[9,15,20] The modules are displayed in Figure 9 and are described in more detail below.

Planar module is composed of membrane plates layered with feed sides facing each other and alternating, where the feed and the permeate sides are separated by a spacer, as displayed at the top of Figure 9. Planar modules are usually highly modular and are stacked in bigger numbers. Theirs packing density (the ratio between the membrane area to its volume) is relatively low, between 100 and 400 m^2/m^3.Planar modules are frequently used in liquid separation.[15,18]

Spiral-wound module: One of the most used modules in gas separation and in CO_2 separation specifically. It consists of flat membranes separated by spacers and sealed. The feed is directed in the axial direction along the module. The permeate flows through the space created by spacers perpendicularly to the feed flow and is directed into the central perforated tube. The whole concept is clearly shown in bottom left of Figure 9. This cross-sectional flow is not as thermodynamically efficient, but width of the channels allows for lowered pressure drop across the module. These modules usually contain multiple membrane sheets stacked together and wrapped around the tube. Among the advantages are high temperature allowance, compactness, wide pressure ranges and its inexpensiveness.[15,18]

Tubular module: Consists of a bundle of tubes inserted inside a tube with a bigger diameter. The feed flows through the small tubes and the separation happens on their walls while the permeate exits through the inside of the outer tube. This module allows for easier fouling control. [15]

Capillary and hollow fiber module: Both these modules are similar in build to shell and tube heat exchangers. A bundle of capillaries is connected at the ends by bonding agents such as epoxy resins or polyurethanes and inserted into a shell tube. Drawing the heat exchanger parallel, the feed can either flow through the capillaries and exit through their walls or it can flow through the "shell" and permeate through the walls outside-inside. Packing densities are much higher than in the case of planar module and range in 600-1200 m^2/m^3. The advantage is an easy fouling control and possible flushing of the module while the disadvantage is that the capillaries can only withstand smaller pressures (4-6 bar). It is mainly used in medicinal scenarios. The hollow fiber module works principally the same only the tubes are smaller. They are self-supporting and resistant to high pressures, which makes them viable to use in gas

separation.[15] Hollow fiber membranes are very sensitive to any solid debris and are difficult to clean so pre-treatment may be required.[18] Bottom right part of **Figure 9** displays the module and **Figure 10** shows hollow fibers under microscope.

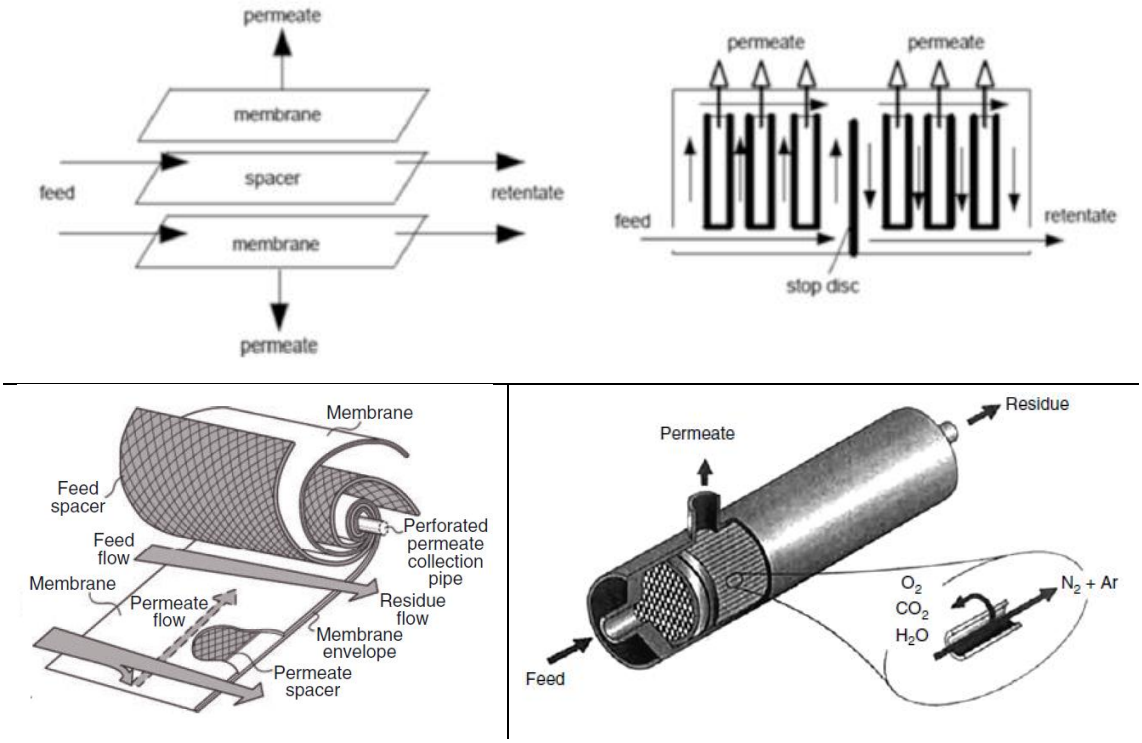

Figure 9. Membrane module configurations. Top: planar module; Bottom left: spiral-wound module; Bottom right: hollow fiber module.[15]

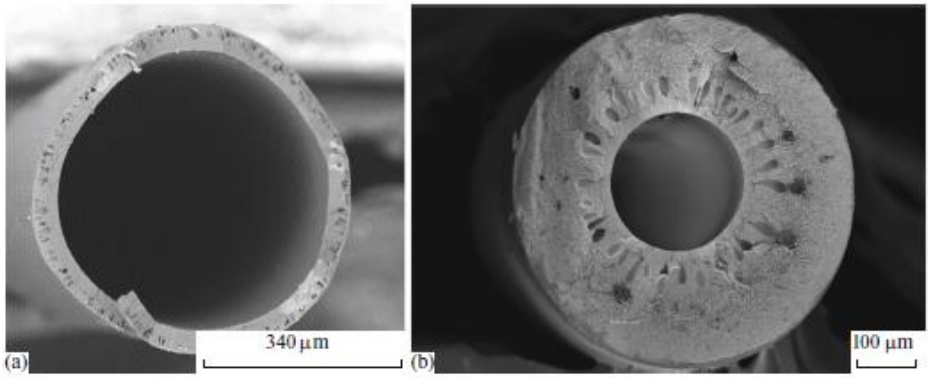

Figure 10. Hollow fibers used in: (a) air separation, (b) separation of He from natural gas.[17]

3.3. Mechanisms of membrane separation

We previously listed different membrane separation principles in **Figure 7**. The main prerequisite for membrane separation is pressure difference between feed and permeate that subsequently causes a difference in dissolved gas concentration, as shown in **Figure 11**. Diffusion happens in these steps:

1) The gas diffuses from polymer surface into the bulk polymer.
2) Gas molecules further diffuse through the polymer matrix.
3) The gas is diffused from the bulk matter to the surface.
4) The desorption of gas from polymer surface to permeate stream.

Permeance (permeability) and selectivity as the main characteristics determine how efficient the separation is. Both terms and their units were described in section 3.1. [15–17] Based on their selectivity and flux, membranes can be divided into: (a) porous and (b) nonporous. [16]

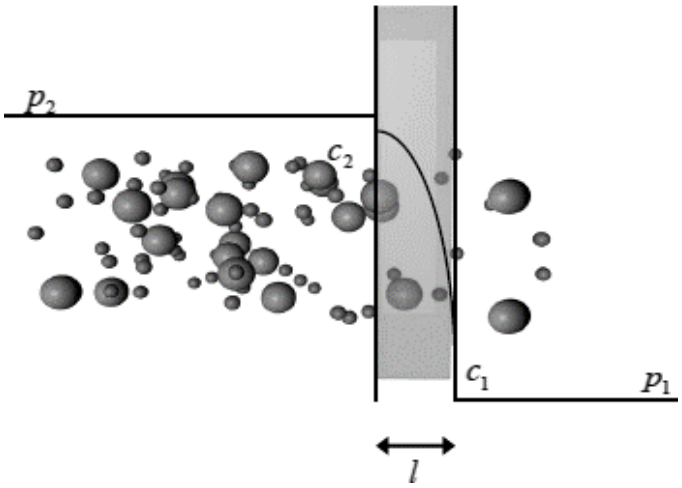

Figure 11. Membrane separation of gases by a non-porous polymeric membrane of thickness *l*. Pressure and concentration difference is the driving force.[16]

3.3.1. Gas transport through porous membranes

Porous materials have hollow structure with randomly dispersed pores. Porous membrane is structurally similar to filters in that, much like the filter only allows for passing of smaller particles, the membrane separates molecules that are significantly different in size.[15] Gas transport through membranes has two components: (i) Knudsen flow and (ii) Poiseuille (or viscous) flow. The ratio between mean free path (λ_i) (eq.XY), and pore radius (r_p) determines

which of the two flows is the prevalent one. If $r/\lambda_i >> 1$, then the transport can be described by the dominant Poiseuille flow as: [16]

$$J_P = (r_p/16L\eta RT)(p_1 - p_2) \quad \text{(eq.7)}$$

where L is the pore length, p_1 is the gas partial pressure in feed and p_2 is the gas partial pressure in permeate. If, on the other hand, $r/\lambda_i << 1$, then the prevalent flow is the Knudsen one. This is because the gas molecules collide with the pore walls way more frequently than they collide among each other. As molecules hit the walls, they are adsorbed for a short period of time and then they rebound randomly. Molecules of different compounds have different speeds and as they move more freely without colliding with other molecules, they get separated. That is the principle of Knudsen flow (J_K) which can be described by the following equation[16]:

$$J_K = (8r_p/3L\sqrt{2\pi MRT})(p_1 - p_2) \quad \text{(eq.8)}$$

which tells us that the flux through the membrane is inversely proportional to the square root of the molecular weight. If the pore size is smaller than 50 nm, the Knudsen separation is possible.[9,15]

In practice, pore sizes are never uniform throughout the material and so instead of one exclusive transport mechanism, there is usually a combination of them. Surface and Knudsen diffusion usually occur in conjunction. [16]

3.3.2. Gas transport through non-porous membranes

Non-porous membranes are quite dense with non-continuous passages (non-porous polymer structure is shown in Figure 12. The main mechanism in non-porous membrane separation is the solution diffusion (shown previously in **Figure 7**).[15] The principle is best understood if we imagine a flat polymer of thickness l that separates two areas filled with gases. Such scenario is shown in Figure 11 – feed gas on the left side maintained at pressure p_2 is separated from product (permeate) side that is maintained at pressure p_1, where $p_2 > p_1$. Under steady state and constant temperature Fick's first law applies and from it, we can define gas permeability P as[16]:

$$P = [(c_2 - c_1)/(p_2 - p_1)]\overline{D} \quad \text{(eq.9)}$$

This equation applies only for permeation of a pure gas, for a gas mixture, pressures *p1* and *p2* need to be replaced with partial pressures of respective compounds in permeate and retentate. In non-ideal gas scenarios (e.g.: high pressure applications) the pressure would be replaced by fugacity. If the feed pressure and concentration is significantly higher than on the permeate side, then the diffusion coefficient does not depend on neither concentration nor time and, thus, can be considered a constant. Under such conditions, equation 9 can be rewritten as[16]:

$$P = c_2/p_2\, D \qquad \text{(eq.10)}$$

and, using Henry's law, we can express permeability of gas *A* as:

$$P_A = D_A S_A \qquad \text{(eq.11)}$$

where D_A is the diffusion coefficient and S_A is the solubility coefficient of component A. S_A is calculated at feed side of the membrane ($S = c_2/p_2$). Based on that, we can say that the permeability depends on two things: (1) thermodynamic component *S* and (2) kinetic component *D*. For example, H_2 as the smallest molecule, has a high diffusion coefficient and CO_2, on the other hand, has a high solubility coefficient.[16] A universally recognized permeability unit is *Barrer*, defined in equation 4. In case of asymmetric membranes for which the thickness is harder to define, *GPU* (gas permeation unit) – defined in equation 3 – is used and it expresses *permeance* also defined in 3.1.[15,16]

The second crucial characteristic of membrane separation is selectivity α, defined as a ratio of permeabilities of gases. Between pure gases *A* and *B*, the ideal selectivity is:

$$\alpha_{A/B} = P_A/P_B \qquad \text{(eq.12)}$$

Usually, the more permeable gas is noted as *A*. Non-porous membranes usually have higher selectivity, even for molecules of similar sizes, as the dominant mechanism is based on different solubilities. Obviously, the ideal scenario would combine high selectivity with high permeability. Figure 13 shows what is called a Robeson diagram – a functionality of permeability vs ideal selectivity. The upper bound line represents the limit to the tradeoff between permeability and selectivity, and is dependent on the molecule's kinetic diameter.[15,16]

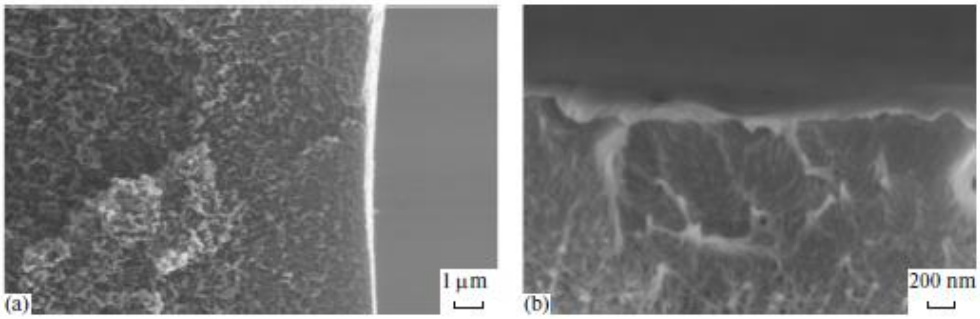

Figure 12. SEM of non-porous membranes for (a) air separation and (b) helium separation.[17]

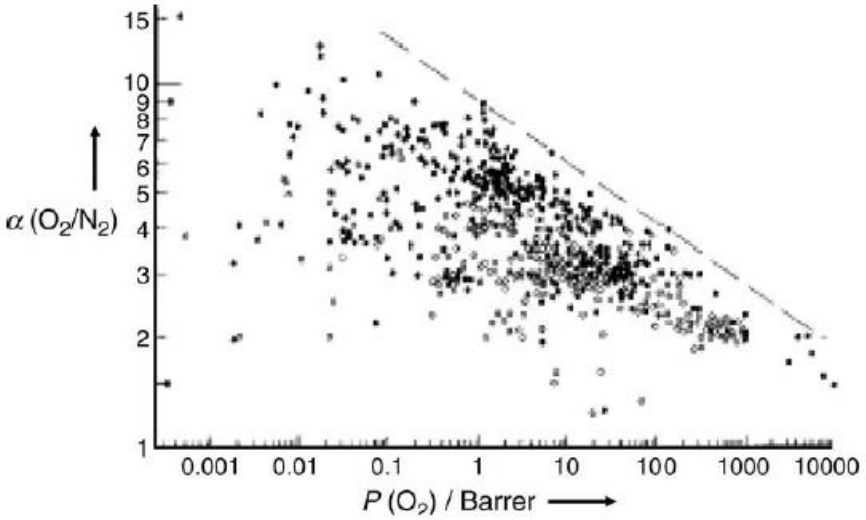

Figure 13. Permeability vs ideal selectivity of several polymers – Robeson diagram.[12]

3.3.3. Gas transport through asymmetric membranes

Asymmetric membranes are used in commercial practice and their properties combine high permeability and solid mechanical strength. In principle, these membranes combine two layers: (1) a thin selective layer (0.1-1 μm) and (2) a thicker microporous supportive layer (50-200 μm). The first layer can be described as non-porous and thus, the main mechanism is the solution-diffusion model. The microporous layer combines Poiseuille and Knudsen flow.[15] However, this combination of flows was found to be present in membranes, where the thin selective layer has a minor portion of defects called pinholes. Ideally, these defects would not exist, and the idea is for the selective layer to be as smooth and uniform as possible.[16] The amount of contribution of these two flows depends on the pore size, porosity and operating temperature and pressure.[15]

3.4. CO_2 membrane separation

After laying out the historical and technological background of CO_2 emission problematic and the theory behind gas membrane separation, we are going to focus more closely on separation of CO_2.

The main debate surrounding CO_2 membrane separation is about determining if permeability or selectivity should be the preferred property. In general, high gas permeance lower the are requirements (and saves initial investment costs) while high selectivity allows for higher CO_2 permeate concentration. For high selectivity, however, high pressure difference is required which brings up the cost of the operation.[9] So there is certainly a certain sweet spot to be found when designing gas separation membranes. We already mentioned the Robeson diagram, which is a staple in evaluating CO_2, and for that matter all gas membrane separation performance. Another interesting tool is a diagram called a performance map shown in Figure 14. It is based on a 1-D mathematical model limited to co-current configurations. These maps (diagrams) show the relation between CO_2 concentration in permeate and the separation efficiency (recovery) (eq.1). Additionally, this diagram is expanded by the use of two more dimensionless criteria - θ and ϕ – the permeation number and the ratio of feed and permeate pressures, respectively[9]:

$$\theta = \frac{\Pi_i P^F A}{x_i^F Q^F} \quad \text{(eq.13)}$$

$$\phi = \frac{P^F}{P^P} \quad \text{(eq.14)}$$

$$\Pi_i = \frac{J_i}{\Delta P_i} \quad \text{(eq.15)}$$

$$\Delta P_i = P_i^F - P_i^P \quad \text{(eq.16)}$$

The permeation number (eq.AF) is the ratio between membrane permeation and the convective transport along the membrane. The ratio of pressures ϕ between feed and permeate sides indicates how strong the separation driving force is. Permeance of component - Π_i – needed to calculate θ, depends on its flux J_i.

Figure 14 maps show a clear trend: at constant pressure ratio ϕ the higher recovery correlates with a lower permeate CO_2 concentration. Increased pressure ratio then means higher permeate CO_2 concentration with the same CO_2 recovery. Therefore, if we had a membrane of known permeance and selectivity and known stream composition (e.g.: known flue gas composition), we could easily get the two parameters - θ and ϕ – necessary to get a permeate stream of required quality. For the left-hand side diagram where the selectivity is equal to 50, we can start from the

bottom section for which the CO_2 feed concentration is 10%; the pressure ratio ϕ equal to 50 and permeance number θ equal to 10 would give us a permeate with around 30% of CO2 and roughly 62% recovery. These two values can be then used in the right-hand side diagram (with selectivity = 250) to determine the necessary operating conditions to keep the permeate quality and overall recovery.[9] The overall idea would be for such diagrams to serve as a starting point in designing a carbon capture process and help with process parameter optimization.

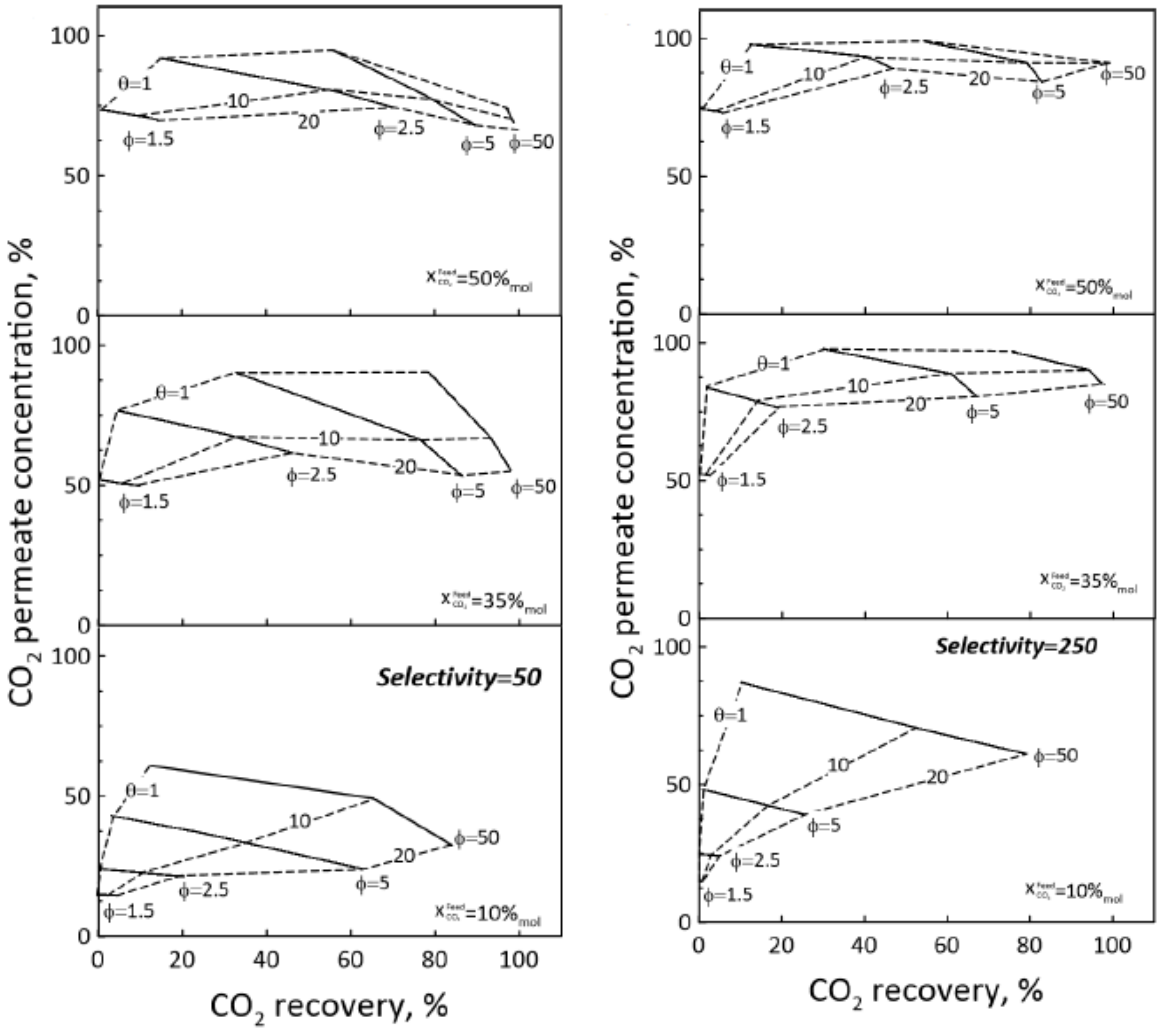

Figure 14. CO_2 membrane separation performance maps – diagrams connecting permeate concentration and CO2 recovery while considering multiple factors such as the permeation number θ. Left hand side diagram shows selectivity at 50 and the right-hand side selectivity is 250.[9]

3.4.1. Polymeric membranes for CO_2 separation

Other than good permeability and selectivity, a polymeric membrane for CO2 separation should also exhibit good thermal resistance. This can be achieved by combining glass and rubbery polymer segments. Among the most studied polymers in this field are polyimides, polyacetylenes, polysulfones, polycarbonates and many more. [12] Figure offers a comparison of different polymers tested at 35°C and 10 atm.[12] Table 5 and Figure 15 offer a comparison of various polymers and their parameters.

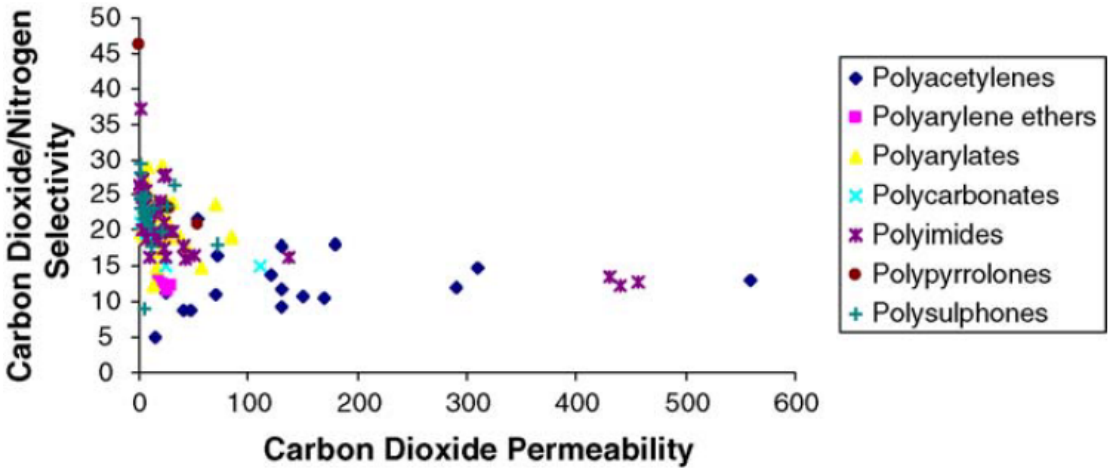

Figure 15. Robeson diagram showing performances of various polymers.[12]

Table 5. Polymeric membranes for CO_2 separation and their properties.[18]

Material	**CO_2/N_2 selectivity**	**CO_2 permeance [$m^3.m^{-2}.Pa^{-1}.s^{-1}$]**
Polydimethylsiloxane	11.4	3200*
Polydimethylphenilene oxide	19	2750
Poly(4-vinylpyridine)/polyetherimide	20	52
Polyethersulfone	25	665
Polyacrylonitrile with ethylene glycol	28	91
Polysulfone	31	450
Polyimide	43	735
Poly(ethylene oxide)	52	52
Poly(amide-6-b-ethylene oxide)	61	608
Polyvinyl alcohol (cross-linked)	170	8278*
Vinyl alcohol/acrylate copolymer – FT	1417	2400*
Polyvinyl alcohol (cross-linked formaldehyde)	1782	338*

Barillas[21] reported on polymeric membranes for CO2/H2 equimolar separation. The membranes were based on PEG-, PTMEG-based membranes with selectivities of around 11 and permeabilties of around 800 and 900.

MMM – Mixed matrix membranes

These membranes are comprised of a polymeric matrix impregnated on anorganic nanoparticles. The polymeric phase is the main one while the anorganic one is dispersed within the polymeric one – principle shown in **Figure 16**. Performance of some notable MMMs is shown in F

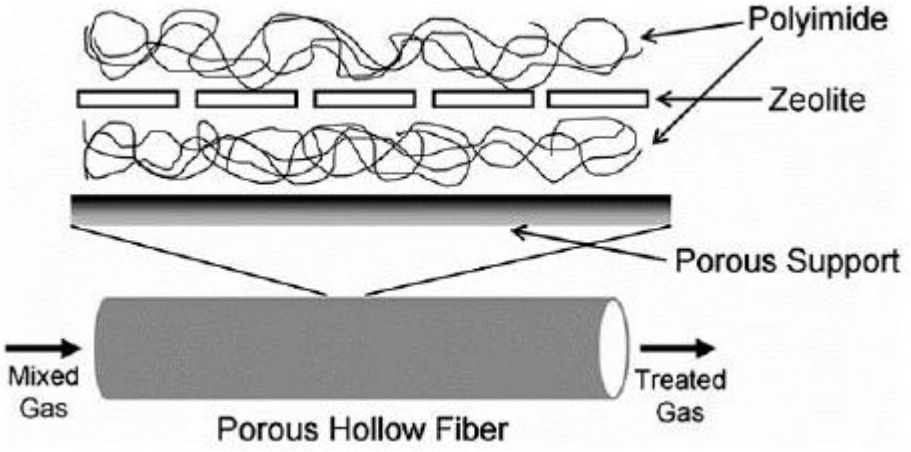

Figure 16. Mixed matrix membrane composition.[22]

Table 6. Separation properties of selected MMM materials.[22]

Continuous phase	**Zeolite**	**c (%mol)**	**Permeability CO_2 (Barrer)**	**Selectivity (CO_2/N_2)**
Polyvinyl acetate			3.1	34.7
Polyvinyl acetate	4A	15	2.4	30.7
Polyvinyl acetate	KFI	20	4.9	53.6
Polyvinyl acetate	H-ZK-5	15	4.9	41
Polyvinyl acetate	Na-SSZ-13	15	4.5	41.7
Polyvinyl acetate	SAPO-34	15	4.4	44.4
Polyvinyl acetate	SAPO-44	15	4.9	51.8

Torstensen[23] reported on PVA/nanocellulose mixed membranes used in CO2/N2 separation. The reported permeance was 128 GPU and CO2/N2 separation factor was equal to 39.

3.4.2. Inorganic membranes

These membranes show good stability at elevated temperatures and much like the polymer ones the inorganic membranes are divided into porous and nonporous. The main transport mechanism is the molecular sieving. Among these materials are zeolites and carbon. inorganic membranes show good affinity towards CO2 and thus show good CO2/N2 selectivities.[4,22]

SAPO-34 membranes

This work[24] reported on SAPO-34 asymmetric tubular membranes. The focus was similar to that of our work – describe the membrane properties under different process parameters. Figure 17 shows the effect of temperature on membrane performance. The paper reported on an 15/85 CO2/N2 permeance (4120 GPU) and 110 selectivity – tests performed at 243 K and 0.1 MPa pressure drop. When temperature was brought to 423 K the 15/85 mixture still achieved impressive numbers – 1390 GPU and 10.3 selectivity. The temperature change is an interesting mechanism – up to a certain point CO2 adsorption is favored by T ramp up but a breaking point is present where the performance drops drastically with further temperature decrease.[24]

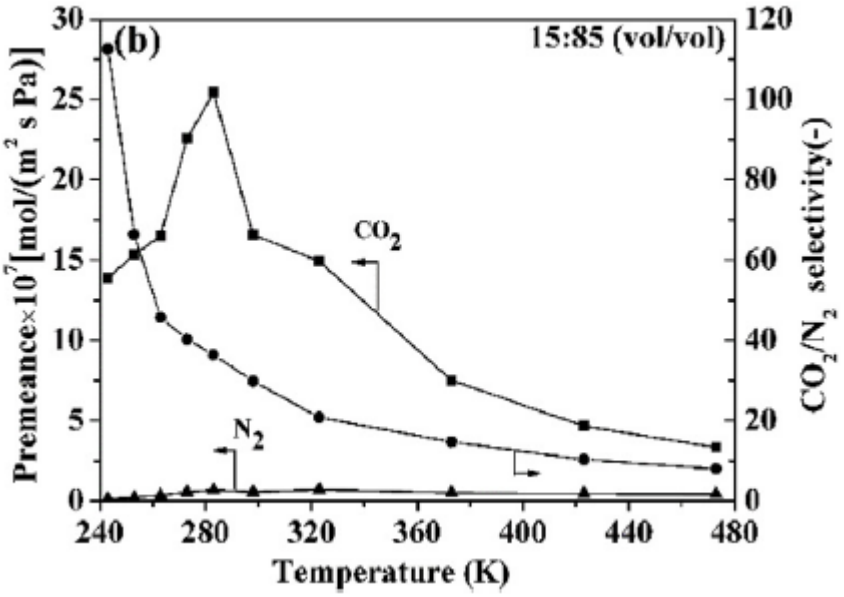

Figure 17. Selectivity and permeance of SAPO-34 based membrane based on process temperature.[24]

4. Experimental part – CO_2 membrane separation

Up to this point, we have described the theoretical background needed to understand the following practical part of this thesis. In the introduction, we laid out the problem of CO_2 emissions and the motive behind the effort to reduce worldwide CO_2 emissions. In section 2, we described how industry sector is the top contributor to greenhouse emissions and explained why CO_2 separation from flue gases is crucial. Moreover, we listed emission composition and introduced the traditional methods of CO_2 separation – absorption, adsorption, and cryogenic distillation – and compared them to membrane separation. In section 3, gas membrane separation was described in more detail including the necessary terminology. Membranes were classified based on their materials and modules and, subsequently, the mechanisms of membrane separation in porous, nonporous, and asymmetric membranes were introduced. In section 3.4 we focused more closely on membrane separation of CO_2, and explored current materials, approaches and reported performances of these membranes. Following pages report on our effort to better describe parameters that influence CO_2/N_2 membrane separation. We focused on these parameters: (1) temperature, (2) pressure, (4) flowrate, and (3) CO_2 concentration. The focus on gas composition is the main contribution of this work as we felt like this dependency has not been studied extensively enough so far. This work can be considered a succession and extension of a master's thesis[25] done by our former colleague on similar topic and we recommend the reader to investigate it.

4.1. Equipment and methods

Recently, our department – the department of process engineering at CTU in Prague – acquired a new membrane separation unit with the intention to dive into this field of research. The unit, its properties and operation are described in following parts.

4.1.1. Membrane unit

The purchased unit was the RALEX GSU-LAB-200 by MemBrain, a company based in Czech Republic. The unit is comprised of the following parts: (1) the membrane module thermostatic box made out of stainless steel and PVC; (2) Bronkhorst thermal mass flow controllers; (3) manual shutoff valves for each line (feed, permeate, retentate, and the individual sampling lines – high-pressure feed, low-pressure feed, permeate, retentate); (4) flexi hose with quick couplings for membrane module attachment; (5) float flow meter; (6) PLC display; (7) EMERSON gas analyzers; (8) distribution box (16 A, 230 V).[26]

The initial installation was done by fixing the hollow-fiber module from the top size of the unit (Figure 18), using the quick couplings and flexi hoses. Dry, clean gases or gas mixtures are required for operation. Steady state is required for data recording, therefore after initial startup it was always necessary to wait for the feed and the temperature to stabilize. The EMERSON gas analyzers cyclically analyze the gas flows. There are six ports for inlet gases - Figure 20. The front size of the unit has three ball valves that are used for a manual feed, permeate and retentate shut off during membrane module exchange - Figure 19. All three figures - Figure 18, Figure 19 and Figure 20 – show unit components, while Table 7 lists them according to their number.[26]

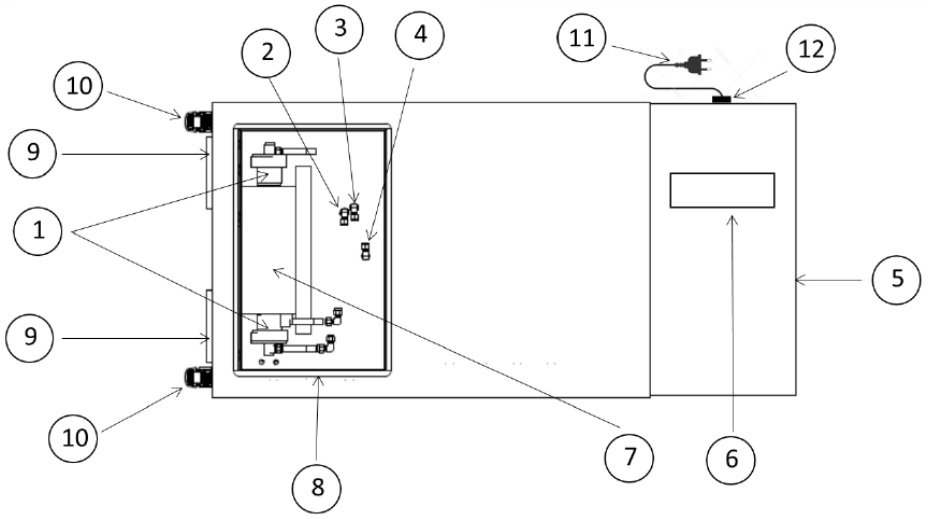

Figure 18. Top view of the membrane unit. Membrane module is placed in the compartment on the left hand side.[26]

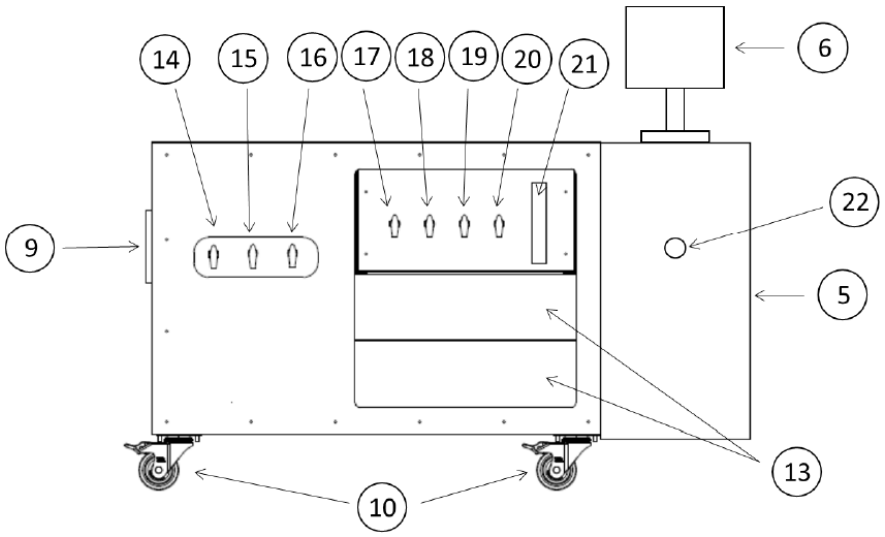

Figure 19. Front side view of the membrane unit.[26]

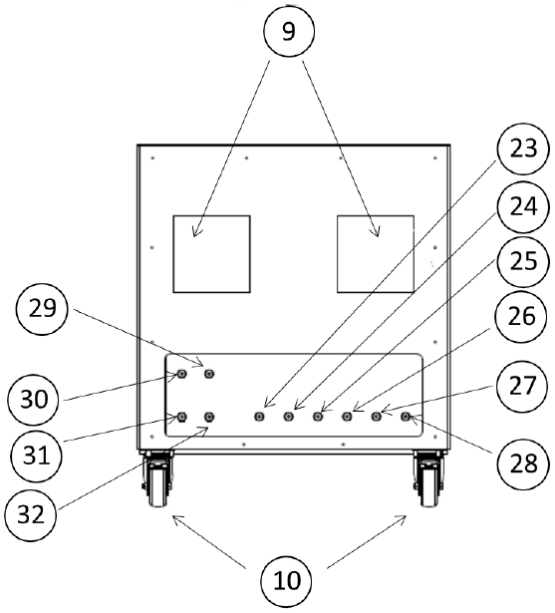

Figure 20. Side view of the membrane unit. It allows for up to six gases to be connected.[26]

Table 7. List of components as shown in previous membrane unit views.[26]

Component number	Component description
1	Membrane module
2,3,4	Flexihose connection in this order: retentate, premeate, feed
5	Electrical distribution box
6	PLC
7	Thermal insulation of module with module heating elements and temperature probes
8	Thermostatic box for membrane module
9	Unit fans
10	Wheels
11	Power cord
12	Ethernet port
13	Analyzers
14, 15, 16	Shut off ball valves: feed, permeate, retentate
17, 18, 19, 20	Shut off ball valves: high pressure feed, permeate, low pressure feed, retentate
21	Mass flow controller
22	Main switch
23, 24, 25, 26, 27, 28	Inlet gas connectors F1 to F6
29, 30 ,31, 32	Process stream outlets: permeate, retentate, sampling system, waste stream

Unit operation

The unit is controlled from the touch PLC (no.6 from the list of components) shown in Figure 21. First, the operating parameters – component flowrates (F1-F6 in the top left part, in blue squares), inlet gas temperature (T1), module temperature (T4). retentate side pressure (P3) and permeate side pressure (P2). Startup phase, in which all set values are being applied and steady state is established after some time, is initiated with the "START" button. In this phase, valve V1 is closed and valve V2 is open so that the gas exits through the waste line ("ODPAD"). Once steady temperature and pressure are achieved, V2 is closed and V1 opened as gas flows through the membrane module (M). Feed, permeate and retentate are analyzed cyclically, based on the

user setup. All input boxes are marked with a "SV" – set value – and actual process parameters are displayed in the "PV" – process value – boxes. The operation process is described in more detail in this[25] work.

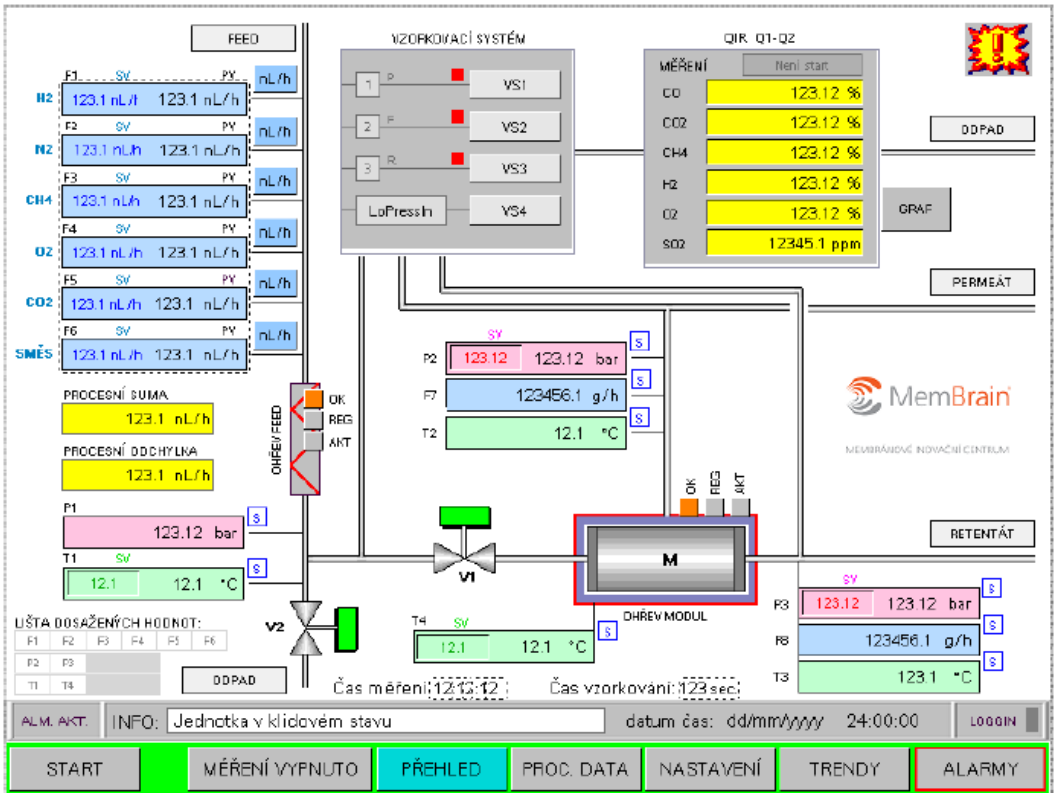

Figure 21. PLC panel initial screen. All parameters during operation were controlled via this interface.[26]

Membrane module

The MemBrain unit was supplied with two different membrane modules – designated P2-1.1 and P2-1.2. Both modules are hollow fiber-type. The thesis previously done on this membrane unit[25] compared the two modules extensively and determined that the P2-1.1 module was not particularly suitable for CO_2 separation as the maximum ideal CO_2/N_2 selectivity achieved during pure gas permeation tests was only about 2.5. Module P2-1.2 on the other hand, achieved an ideal selectivity around 10-times higher.[25] It was therefore decided upon that for our experiments, whose focus was CO2 separation and effect of CO_2 concentration on separation performance, only the P2-1.2 module would be used. Table 8 shows the module's parameters. Considering the fiber material, we can classify this membrane as a non-porous polymeric membrane – the transport mechanism was described in section 3.3.2. The module scheme with

all the connections is shown in Figure 22, the advantages and distinctions of hollow fiber modules was described in section 3.2.2.

Table 8. Properties of P2-1.2 hollow fiber module used in our experimental work.[27]

Parameter	**Value**
Module material	PVC-U
Flange material	PVC/steel
Connecting material	steel
Seal material	rubber and PTFE
Module length	400 mm
Effective area	0.8 m^2
Module inner diameter	28.4 mm
Inlet pressure	0 to 10 bar
Working temperature	0 to 60 °C
Number of fibers	2900
Fiber length	300 mm
Fiber outer diameter	0.3 mm
Fiber inner diameter	0.18 mm
Fiber material	polyetherimide + polyimide

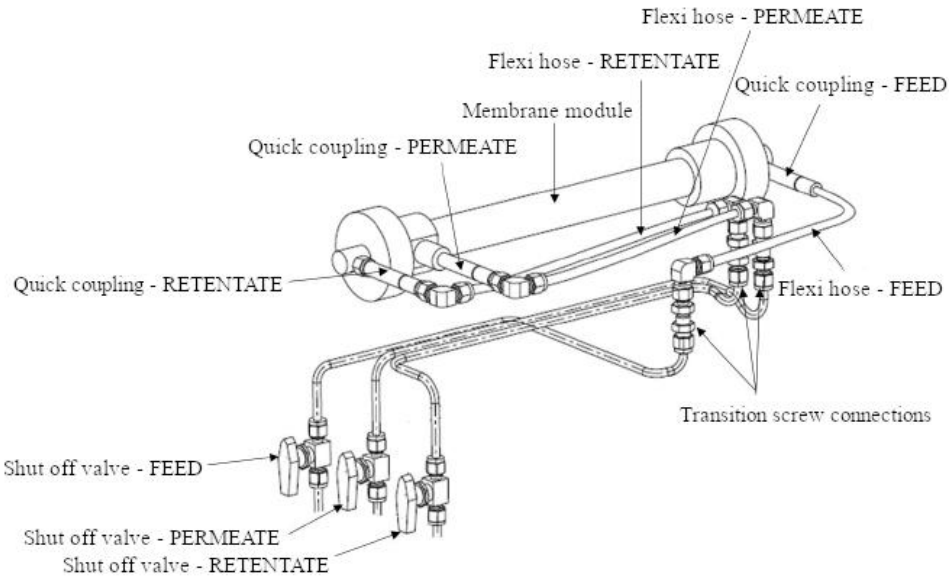

Figure 22. Module scheme including all feed, permeate and retentate connections.[26]

4.1.2. Design of experiments

The parameters we set to explore were temperature, pressure, feed flowrate, and most importantly, CO_2 concentration in feed. Table 9 shows the initial design of experiments (DOE). We aimed to evaluate the effect of changing CO2 feed concentration, changing gas temperature, different gas flowrates all in conjunction with varying pressure differences between retentate and permeate side. The initial design of experiment is shown in Table 9.

Two temperature values were chosen – 21 °C as normal temperature and strictly a baseline value used for reference; 60°C as we wanted to get closer to elevated temperatures real flue gas might have and this was the upper limit of our membrane module. For permeate-retentate pressure difference, the permeate side was fixed at 2 bar while the retentate side started at 5 bar and increased in arbitrary steps of 1 bar until it reached 10 bar. For flowrate variation, 150 and 200 g/h values were chosen. The composition of feed (simulated flue gas) was set according to typical flue gas compositions in coal-fired plants (Table 1), where only the 3 main components were used -N_2, CO_2 and O_2 - and the CO_2 concentration ranged from 5-25%.

It is worth noting that, compared to the design temperature of 60 °C, the actual temperature was usually 55°C, and similarly for other designed values, the actual value was usually different. Nevertheless, all experiments were done under steady state and the actual values are shown in our results. The deviations from the DOE are therefore only a minor inconvenience.

Table 9. Design of experiments. Primary focus of this work was on describing the effect changing CO_2 feed concentrations has on the separation performance.

Temperature [°C]	**Δp [bar]**	**$\dot{m}_{feed}$ [g/h]**	**CO_2 vol%**	**N_2 vol%**	**O_2 vol%**
Pure gas (CO_2 and N_2) – changing flowrate, pressure, and temperature					
21/60	3-8	150/200	100	0	0
21/60	3-8	150/200	0	100	0
Simulated flue gas – changing flowrate, CO_2 concentration, Δp, and T					
21/60	3-8	150/200	5	91	4
21/60	3-8	150/200	10	86	4
21/60	3-8	150/200	15	81	4
21/60	3-8	150/200	20	79	4

21/60	3-8	150/200	25	71	4

4.1.3. Experiment procedure and data processing

Due to safety hazards, the room containing the membrane unit had to be well ventilated – at concentrations >5% CO_2 causes respiratory acidosis and at >10% it may cause lead to loss of consciousness and subsequent death.[28] After startup, the system was flushed with pure nitrogen and the parameters were set: (1) temperature – module and gas – until its stabilization, (2) feed composition, (3) inlet gas flowrates, (4) permeate and retentate pressures. After steady state had been reached, the data recording began. If any corrections had to be made, the manual valves were used. The usual sampling time was 300 s after which the unit was depressurized. The data were recorded automatically and saved in a .csv format. The computer records and saves each parameter dataset in a separate file, therefore those needed to be unified in a single file to be processed.

First, pure gas separation measurements were done, as these were crucial for later comparison to gas mixtures – the data is shown in Table 10. Second, the gas mixture measurements were done - Table 11. It is worth noting that due to high membrane module sensitivity towards CO_2, the pressure differences used in CO_2 measurements were lower than those used in pure N_2 measurements.

Table 10. Data acquired for pure N_2 separation testing at 55°C and 200 g/h.

ideal flowrate	200	g/h	
temperature	**55**	°C	
pressure permeate (bar)	**pressure retentate (bar)**	**flowrate permeate (g/h)**	**flowrate retentate (g/h)**
2.0	5.0	15.2	184.8
2.0	6.0	21.2	178.8
2.0	7.0	26.8	173.2
2.0	8.0	33.6	166.4
2.0	9.0	40.8	159.2
2.0	10.0	48.1	151.9

Table 11. Data acquired for gas mixture with 15.6 vol% CO_2, 150 g/h flowrate at 24.5 °C temperature.

ideal flowrate	150	g/h		mCO2	36.3	g/h	
temperature	24.5	°C		mN2	84.75	g/h	
O2	4.35	(% vol.)		mVZ	28.8	g/h	
CO2	**15.59**	(% vol.)		total	*149.85*	g/h	
pressure permeate (bar)	**pressure retentate (bar)**	**flowrate permeate (g/h)**	**flowrate retentate (g/h)**	**O2 permeate (% vol)**	**O2 retentate (% vol)**	**CO2 permeate (% vol)**	**CO2 retentate (% vol)**
2.0	5.0	17.20	132.60	7.10	4.06	32.48	13.86
2.0	6.0	23.80	126.10	7.36	3.87	35.19	12.63
2.0	7.0	30.50	119.30	7.51	3.67	36.60	11.31
2.0	8.0	37.20	112.80	7.59	3.45	37.12	9.97
2.0	9.0	43.50	106.40	7.62	3.22	36.96	8.60
2.0	10.0	49.20	100.50	7.61	3.00	36.34	7.42

4.1.4. Separation performance calculation

Sorted data from previous steps were unified in a single file and MS Excel was used in following calculations – Table 12 shows an example of calculation results.

Under the low pressures and temperatures used in our experiments, we assumed the ideal gas behavior. This assumption allowed us to equate the molar concentration to the volumetric concentration:

$$c_i^n = c_i^V \qquad \text{(eq.17)}$$

Based on molecular masses of participating gases, and the known permeate and retentate gas composition, we can write:

$$M_{mix} = \sum c_i^n M_i \qquad \text{(eq.18)}$$

or, specifically for our mixture in permeate (and similarly for feed):

$$M^P = \frac{c_{N2}^P}{100} M_{N2} + \frac{c_{CO2}^P}{100} M_{CO2} + \frac{c_{O2}^P}{100} M_{O2} \qquad \text{(eq.19)}$$

$$M^F = \frac{c_{N2}^F}{100} M_{N2} + \frac{c_{CO2}^F}{100} M_{CO2} + \frac{c_{O2}^F}{100} M_{O2} \qquad \text{(eq.20)}$$

Knowing the above, we can calculate the permeate molar flowrate (using the mass flowrate from the measured data) and CO_2 permeate (feed) molar flowrate:

$$\dot{n}^P = \frac{\dot{m}^P}{M^P} \quad \text{(eq.21)}$$

$$\dot{n}^F = \frac{\dot{m}^F}{M^F} \quad \text{(eq.22)}$$

$$\dot{n}^P_{CO2} = \dot{n}^P \frac{c^P_{CO2}}{100} \quad \text{(eq.23)}$$

$$\dot{n}^F_{CO2} = \dot{n}^F \frac{c^F_{CO2}}{100} \quad \text{(eq.24)}$$

and from the CO2 permeate flowrate, the molar flux can be obtained as:

$$J_{CO2} = \frac{\dot{n}^P_{CO2}}{3600\ A_{mem}} \quad \text{(eq.25)}$$

From there, the permeance (based on equation 15) can be calculated as:

$$\Pi_{CO2} = \frac{J_{CO2}}{\Delta p_{CO2}} \quad \text{(eq.26)}$$

and using equation 3, the obtained value can be divided by $3.35x10^{-10}$ to get the GPU permeance value.

With known membrane fiber wall thickness *l*, permeability can be calculated:

$$P_{CO2} = \Pi_{CO2} \cdot l \quad \text{(eq.27)}$$

and subsequently expressed in Barrer by dividing the previous value by eq.4. In case of pure gas separation, the membrane selectivity is characterized by its ideal selectivity of gas pairs as:

$$\alpha_{CO2/N2} = P_{CO2}/P_{N2} \quad \text{(eq.28)}$$

With gas mixtures such as our simulated flue gas, the membrane selectivity can be expressed using the separation factor:

$$S^F_{CO2/N2} = \frac{y^P_{CO2}/y^P_{N2}}{y^R_{CO2}/y^R_{N2}} \quad \text{(eq.29)}$$

Recovery, otherwise known as separation efficiency, is calculated according to equation 1 as:

$$\eta_A = \dot{n}^P_{CO2}/\dot{n}^F_{CO2} \quad \text{(eq.30)}$$

4.2. Results and discussion

4.2.1. Single gas performance

Pure gas separation using CO_2 and N_2 was done to better show the properties of the unit and also to build on previous works[25] that characterized it but solely for one temperature value. Pure gas permeabilities and selectivities are mostly used in research to characterize membranes, however, many times, these are limited to only fixed parameters. In our single gas permeation tests, we aimed at showing how changing the process temperature has a significant effect on the separation performance. Moreover, we wanted to compare pure gas permeances to gas mixture permeances and thus show, that membrane characteristics based on pure gas permeabilities and selectivities might not be the best practical tool – as most real-world membrane uses treat gas mixtures. Throughout the experimental part, we focused on the CO_2/N_2 separation as this is the prevalent one in flue gas CO_2 separation.

Table 12 shows results of calculations showed in section 4.1.4 for pure N_2 separation done at 55 °C and 200 g/h (data shown in Table 10). We mainly focused on the staple membrane separation characteristics such as permeance, recovery and separation factor.

First, we showed how permeance depends on the partial pressure difference between the feed side and the permeate side (in case of pure gas separation, the partial pressure equals the total pressure) – the results are shown in Figure 23. The figure shows that CO_2 permeance increases with increasing pressure difference while N_2 values remain relatively unchanged. The figure is a bit biased though, as we used lower pressure differences for CO_2 because of the membrane module sensitivity to this specific gas. If were to continue the CO_2 permeance for a higher pressure drop range, the functionality might have shown a more linear trend. A more important behavior, however, is the dependence of permeance on process temperature, specifically in case of CO_2. N_2 did not seem to be affected by temperature as much, CO_2 on the other hand showed approximately 1.5-fold increase in permeance when we shifted the temperature from 25 °C to 55 °C. We think this is due to increased dissolution that accompanies increase in temperature. As the membrane is polymeric, the main mechanism is the solution-diffusion model. This effect should have a thermodynamic limit (as shown in this work[24] with absorption) so it would be interesting to test this further for higher temperatures – something our module does not allow.

We continued by showing the dependence of recovery on partial pressure - Figure 24. The trend was similar, with improved recovery showed using higher temperature. According to equation 30, it depends on molar flows on permeate and retentate side, and if recovery increases

so must the ratio. The improvement most probably has the same origin – more favorable polymer absorption of both N_2 and CO_2. In case of CO_2, the ramp up is steeper, meaning for the same recovery value, we needed a lower pressure difference with increased temperature.

Figure 25 shows the dependency of permeance on partial pressure difference but at the same time compares values from single-gas tests with our gas mixture experiments (the mixture feed contained 4% of O_2, 4.5 % of CO_2 and the rest was N_2). Logarithmic scale was used for pressure difference for better readability. The N_2 permeance was not drastically different. The CO_2 was affected significantly as the mixture showed a downward trend. This is proof that the mixture components significantly affect each other's permeance and so membrane evaluations based on pure gas experiments might sometimes be misleading.

Table 12. An example of calculated values based on measurements from Table 10 for pure N_2 separation; 55°C and 200 g/h.

$M_{P(R)}$ [g/mol]	Q_{per} [mol/h]	Q_{ret} [mol/h]	Q_{feed} [mol/h]	η_{N2}	J_{N2} [mol/m^{2}s]	ΠN_2 [GPU]	P [barrer]
28.0	0.5	6.6	7.142857	7.6	0.000188492	1.87554	112.5325
28.0	0.8	6.385714	7.142857	10.6	0.000262897	1.96191	117.7149
28.0	1.0	6.185714	7.142857	13.4	0.000332341	1.98412	119.0476
28.0	1.2	5.942857	7.142857	16.8	0.000416667	2.07296	124.3781
28.0	1.5	5.685714	7.142857	20.4	0.000505952	2.15757	129.4547
28.0	1.7	5.425	7.142857	24.05	0.000596478	2.22566	133.5398

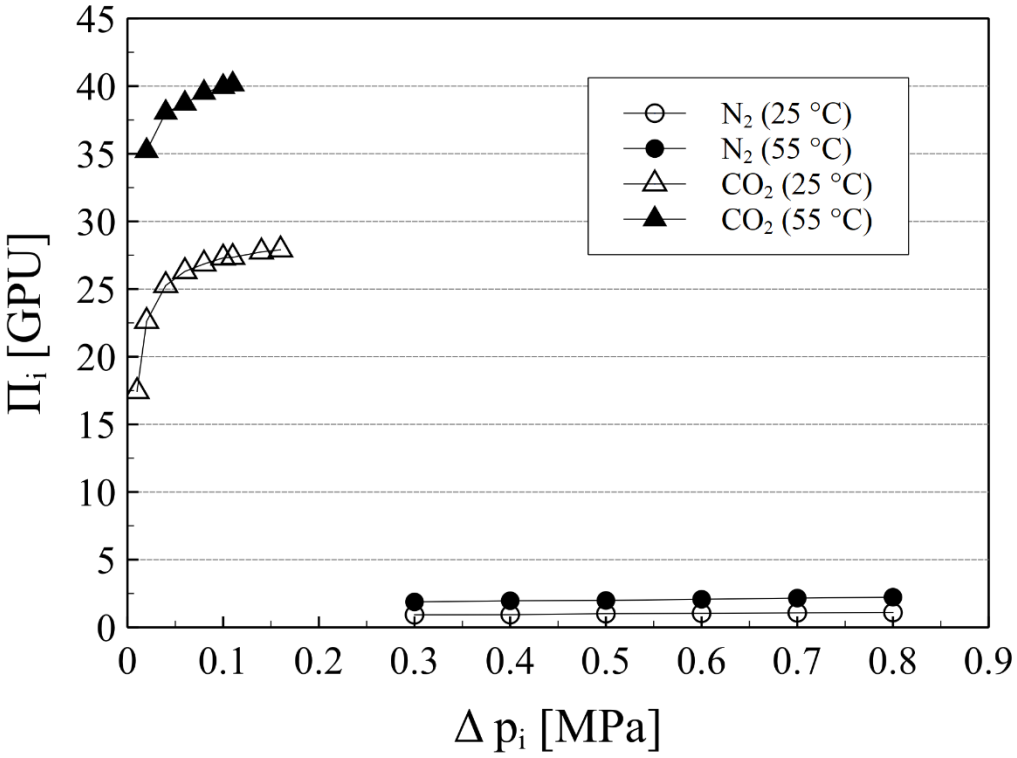

Figure 23. Membrane gas permeance as a function of gas partial pressure difference (driving force). Measurements were done for 25 °C and 55°C with the higher temperature showing better permeance results. Feed mass flowrate was 200 g/h.

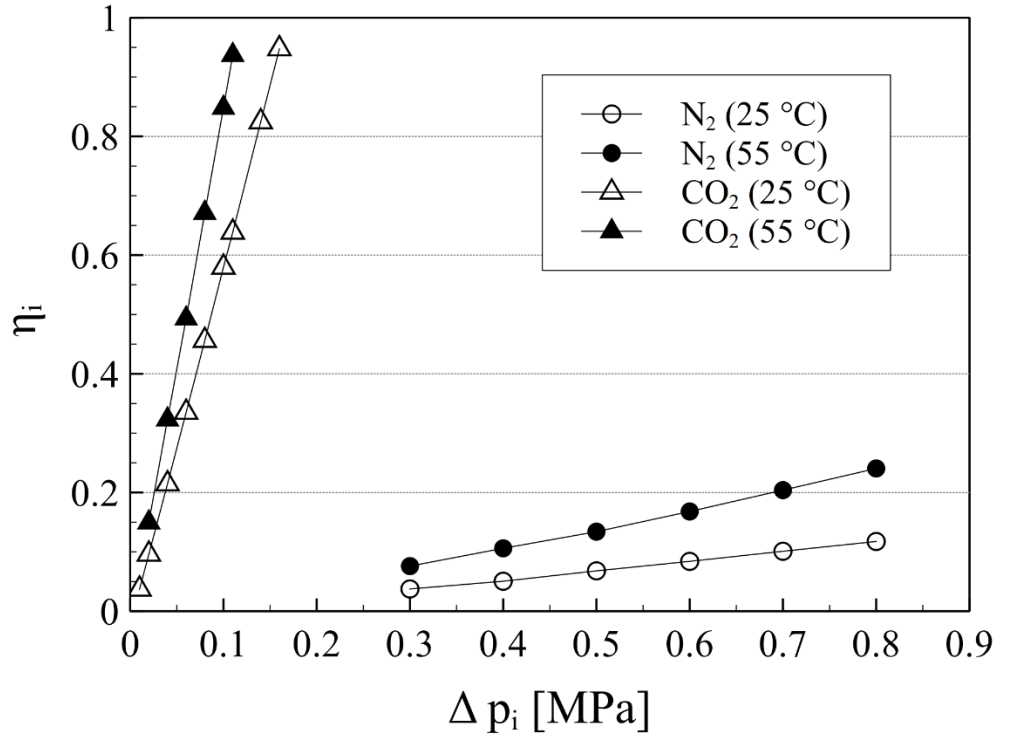

Figure 24. Gas recovery as a function of gas partial pressure difference (feed – permeate). Both N_2 and CO_2 showed better recovery when elevated temperature of 55 °C was used. Feed mass flowrate for these tests was 200 g/h.

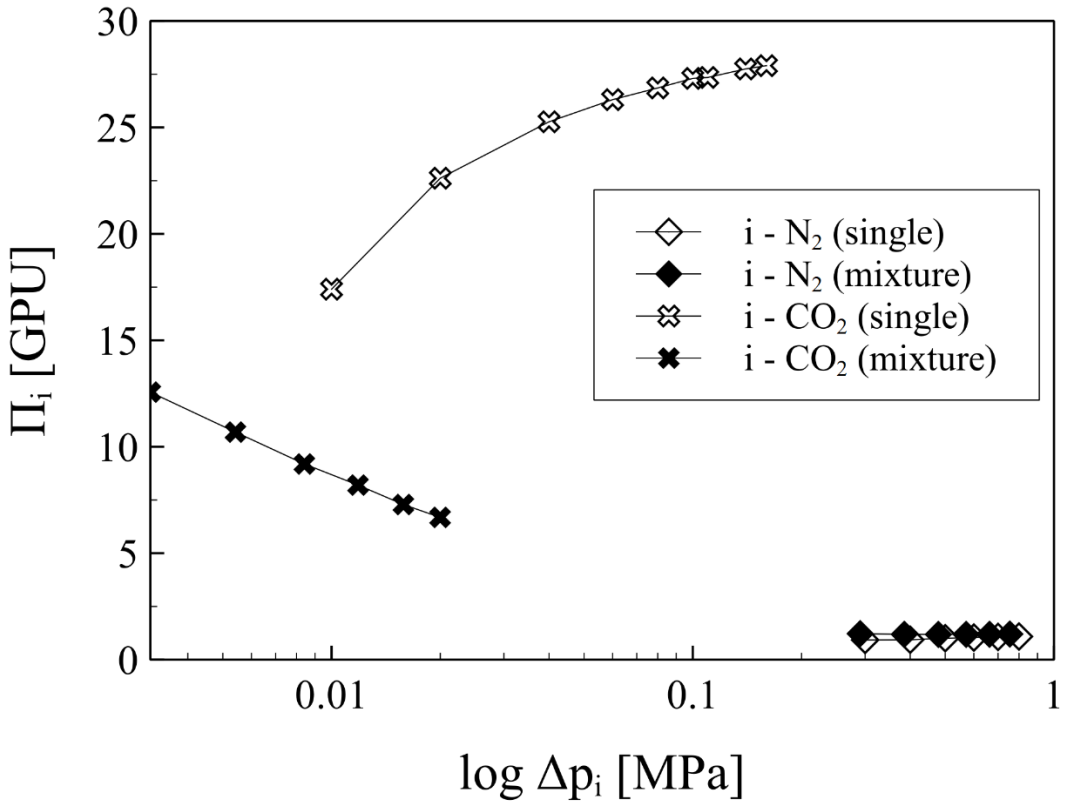

Figure 25. Permeance vs gas partial pressure difference (feed – permeate). This figure compares single gas and gas mixture permeances tested at 25 °C. Permeance of N_2 was not affected significantly while permeance of CO_2 showed vastly different results.

4.2.2. Simulated flue gas separation performance

Previous sub-section was focused on showing the effect of changing process parameters on pure gas permeance and recovery while also comparing pure gas to gas mixture permeance. In this and following sub-sections, we describe the primary goal of this paper – the effect of changing process parameters on CO2 membrane separation from gas mixtures. The gas mixture used here is a simulated flue gas from a coal-fired plant. Typical flue gas compositions were shown in Table 1 and Table 2. In our experiments CO2 feed composition ranged from 5% to 25% volumetric to cover the whole range – the DOE is shown in Table 9. Other that CO2 concentration, the necessary changing parameter was the pressure drop as it is the main driving force behind membrane separation, furthermore, we covered changing temperature, and changing mass flowrate of inlet gas. An example of calculation results is shown in Table 13

Table 13. Selected quantities calculated for a gas mixture experiment; flowrate of 150 g/h , temperature 25°C and 4.3 % CO_2 in feed.

$M_{permeate}$ [g/mol]	M_{feed} [g/mol]	Q_{pCO2} [mol/h]	J_{CO2} [mol/m^{2}s]	Π_{CO2} [GPU]	P_{CO2} [barrer]	S_F (CO_2/N_2)	η_{CO2}
29.7932	28.8672	0.038188	1.32598E-05	12.56556	753.9336	2.653066	17.05
29.98	28.8672	0.055892	1.94069E-05	10.6884	641.3037	3.129083	24.96
30.1008	28.8672	0.074574	2.58939E-05	9.190871	551.4522	3.516489	33.30
30.1828	28.8672	0.093669	3.2524E-05	8.19989	491.9934	4.500479	41.83
30.216	28.8672	0.11114	3.85902E-05	7.286189	437.1713	5.139553	49.63
30.2312	28.8672	0.128822	4.47298E-05	6.682775	400.9665	5.872738	57.52

Effect of changing concentration

The changing CO2 concentration in feed does not have a straightforward effect, as seen in Figure 26. At first thought, one would expect the increased pressure drop to have a positive effect on permeance, but the opposite is the case. As mentioned before, in case of gas mixtures the individual components affect one another's permeance. From equation 26, we see that CO2 flux and its partial pressure are in play. Partial pressure is in turn dependent on CO2 concentration. As we increase the driving force, we promote CO2 flux but also other gases' fluxes. It then becomes a question of membrane material and its favorability of one gas over another – aka selectivity. What is also not straightforward is the effect of changing concentration of CO2 – the trend seems to be roughly linear and declining. Also, there seemed to be a maximum recurring at 15 % CO2. The overall permeance values were fairly small compared to modern commercial membranes.

What is clear is that CO2 partial pressure shows the dependency better than total pressure difference – as shown in Figure 27. The figure shows that with increasing partial pressure difference the permeance decreased - lower CO2 feed concentrations mean steeper permeance

drop-off. In subsequent figures we returned to characterization by total pressure difference as it is the one that we would control in real-world processes.

Figure 28 shows how the CO2 concentration change affects the CO2 recovery. With increasing CO2 %, the recovery went up too. At the same time, the increasing pressure drop helped increase the recovery values.

A similar trend was observed in relation to the separation factor dependency on CO2 % change – as shown in Figure 29. This follows the principle of separation factor – the higher the feed CO2 concentration, the more favorable permeation towards CO2 versus N2. It also shows that the separation factor increases with rising pressure drop. This effect is the opposite of the one described in Figure 26 and Figure 27, where we observed permeance decrease with increasing Δp.

This effect is expected, and we already described it in the theoretical part, there is a tradeoff between membrane selectivity (separation factor) and its permeability (permeance). Therefore, whenever designing membrane separation and picking the right material and configuration, it is an essential question – does the process require higher selectivity (purer permeate) or higher permeance? We tried to characterize this membrane based on its concentration-dependent performance in Figure 30. It is an equivalent to a Robeson diagram showing the dependency of separation factor on permeability. The points are sorted according to CO_2 concentration and driving force and all of them were taken from experiments done at 25 °C and 150 g/h flowrate. Both Δp and CO2 concentration had a significant effect on the points' placement within the graph.

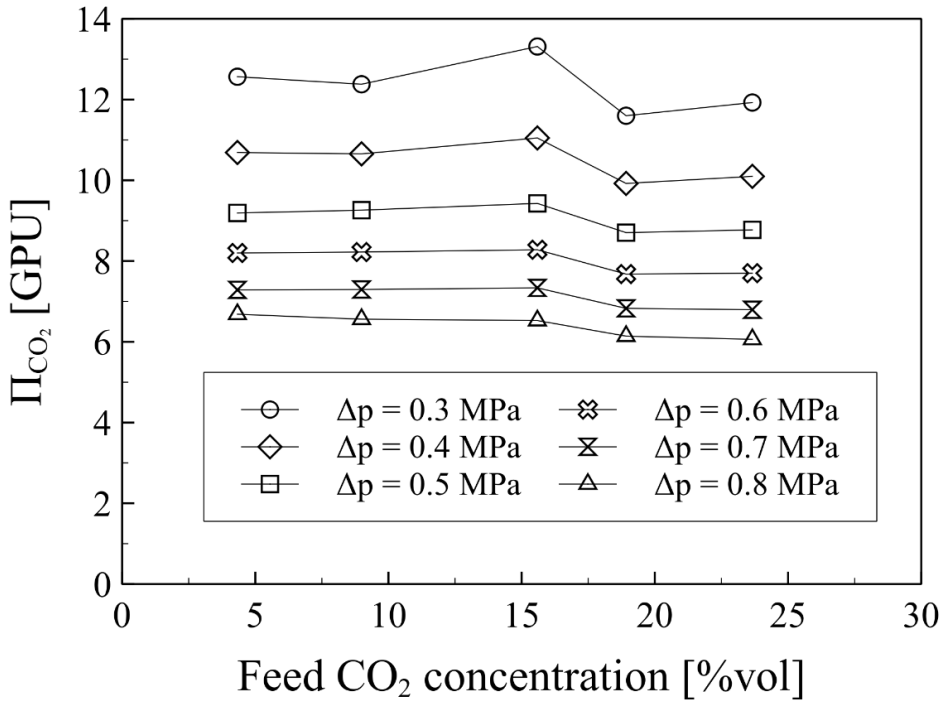

Figure 26. Permeance vs changing CO_2 concentration in feed. In case of CO2, higher pressure differences showed lower permeances, while the concentration change itself did not affect the permeance as much. In general, the overall permeances were quite low. Experiments shown here were done at 25 °C and 150 g/h feed flowrate.

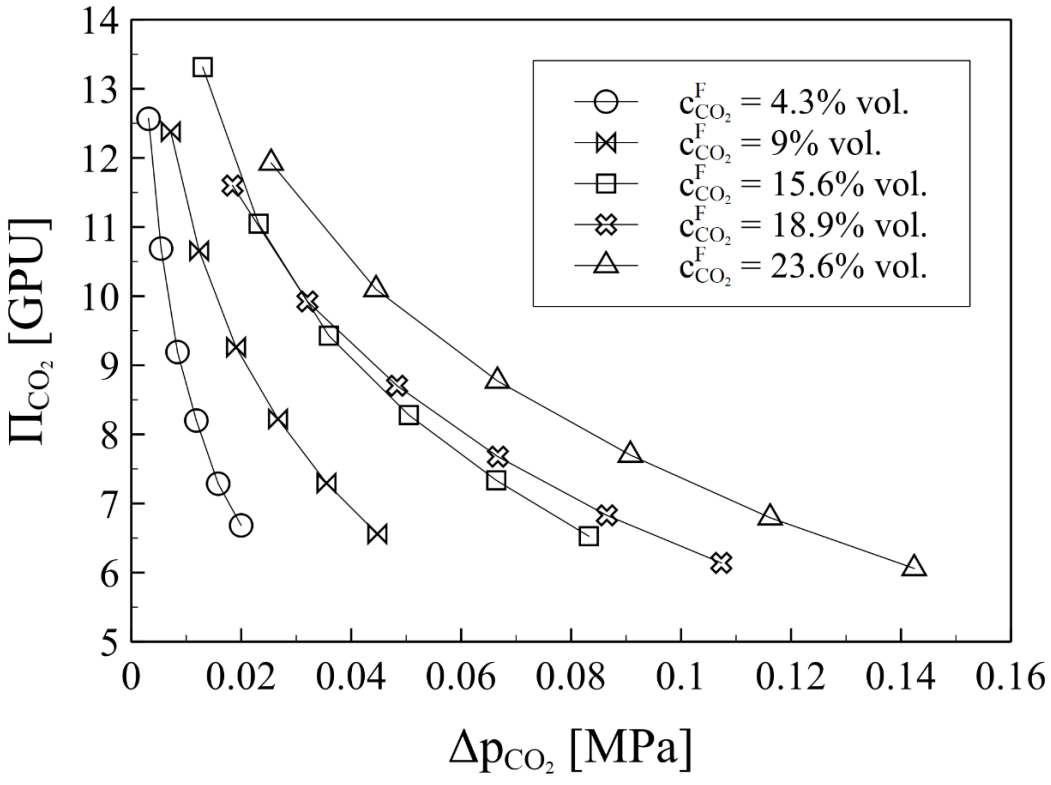

Figure 27. Permeance as a function of partial pressure difference for CO_2. Rising partial pressure difference (feed – permeate) showed decreasing permeance. Using partial pressure instead of total pressure difference is clearer but in terms of process parameter control, total pressure is the one we can control.

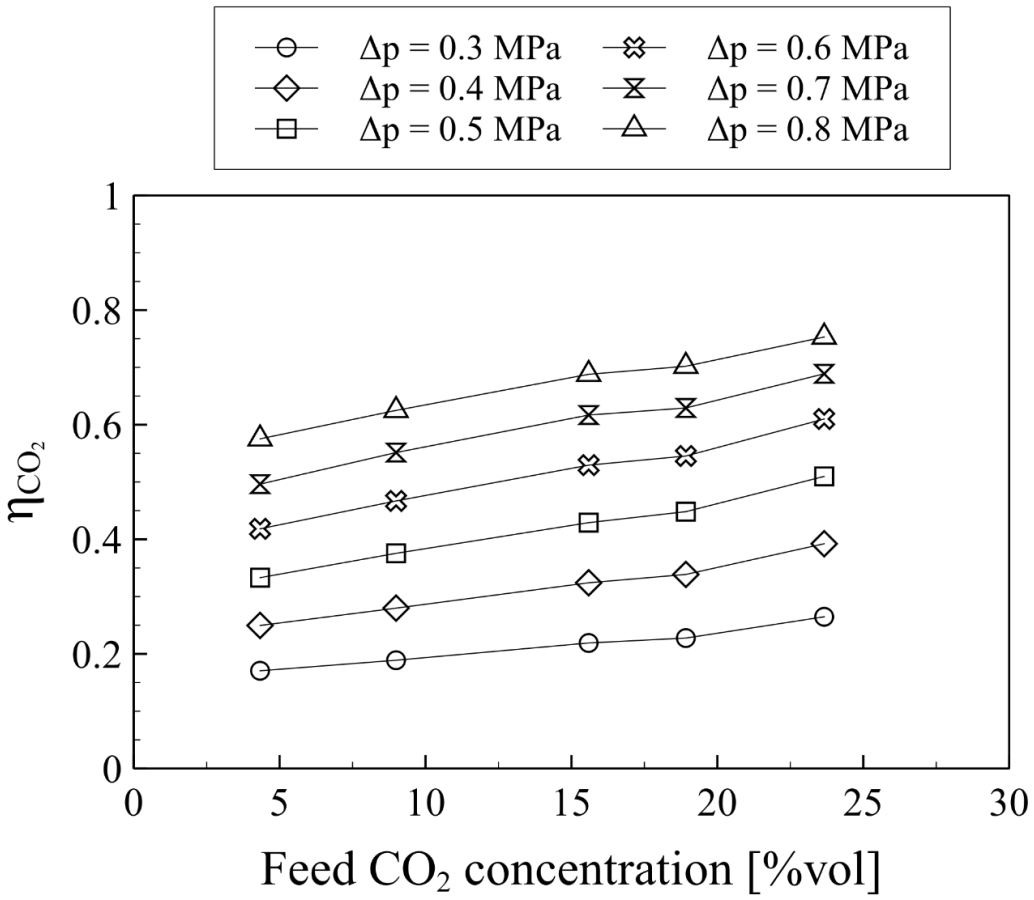

Figure 28. CO_2 recovery vs feed CO_2 concentration. Recovery showed rising tendency with increasing CO2 concentration. The main factor, however, is still the pressure difference.

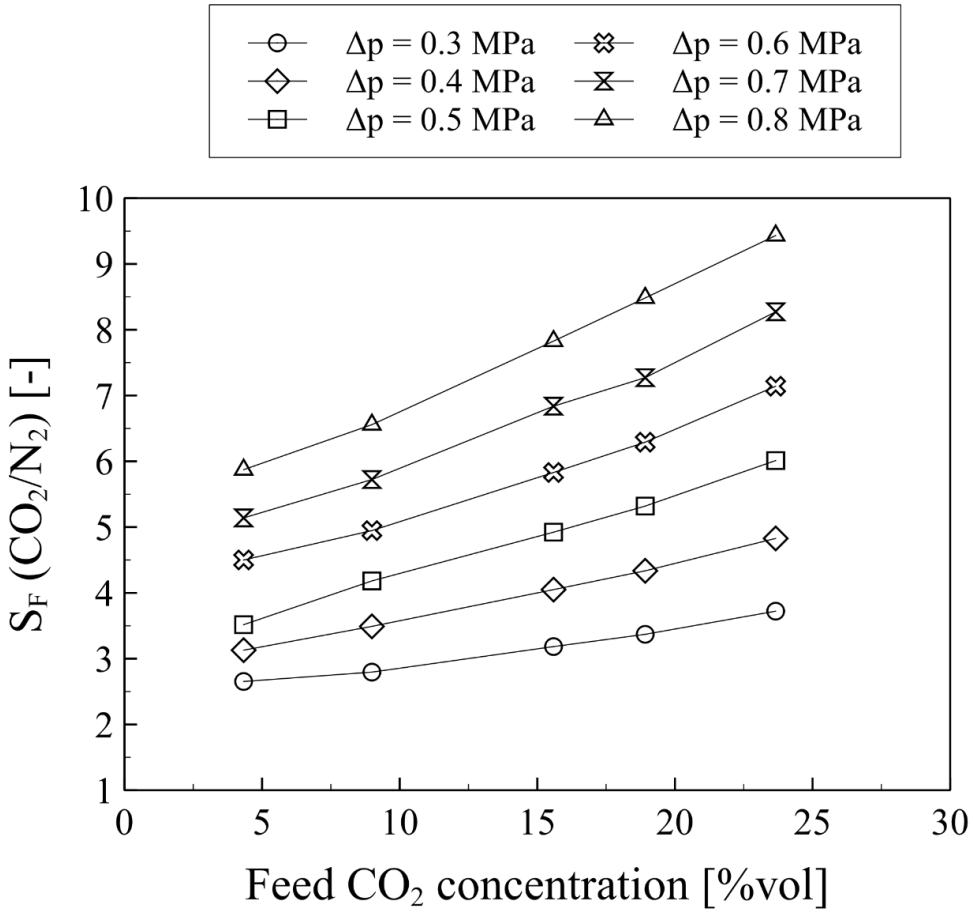

Figure 29. Separation factor as a function of changing feed CO_2 concentration. Unlike permeance, the separation factor increases with higher CO_2 feed concentrations.

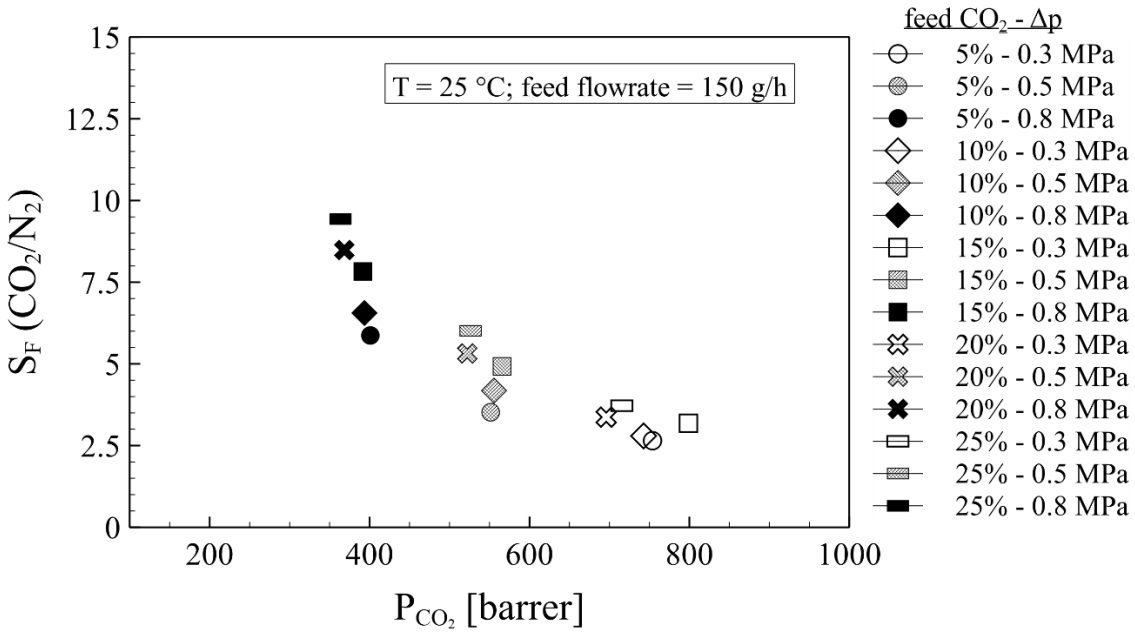

Figure 30. Separation factor vs permeability of tested gas mixture. This diagram is de-facto a Robeson diagram equivalent for our case – we characterized our membrane module using minimum and maximum pressure differences.

Effect of changing temperature and flowrate

Figure 31 shows how temperature change affects the permeance vs CO_2 concentration dynamic. In all cases, the increase from 25 °C to 55 °C showed permeance improvement. As we increased the process temperature, the dissolution of CO_2 into the polymer probably intensified and allowed for better permeance. This effect is expected to have a limit and this limit is going to be different for different materials but most importantly for different gas compositions. In previous research[24], when zeolites were used, the peak temperature after which the temperature increase had detrimental effect was around 12 °C but for binary N_2/CO_2 gas mixture. A similar effect can be observed in Figure 32 where temperature increase has a positive effect on CO2 recovery in the mixture. In case of Δp = 0.8 MPa and 55 °C a 0.9+ recovery was achieved.

Figure 33 shows the effect of feed flowrate ramp up on CO_2 recovery – as we increased the mass flowrate to 200 g/h we observed decreased recovery. This is probably due to oversaturation of membrane surface with gas volume indicating there should be an optimal gas flow for specific membrane areas.

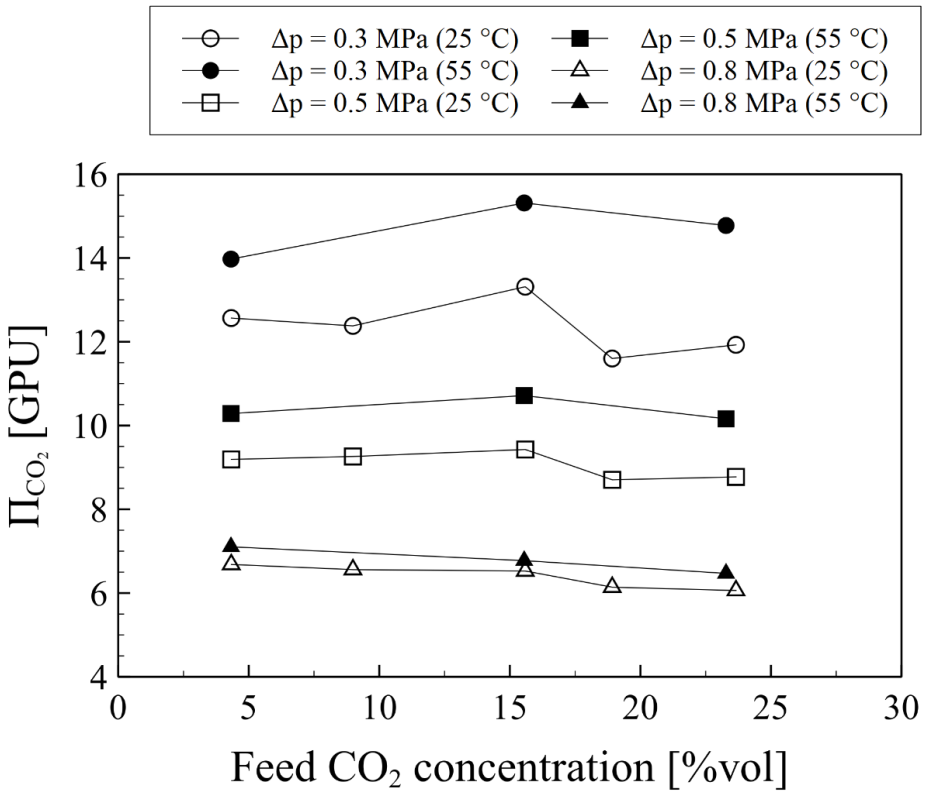

Figure 31. Permeance vs feed CO_2 concentration with changing temperature. Higher temperatures showed improved permeance in all cases.

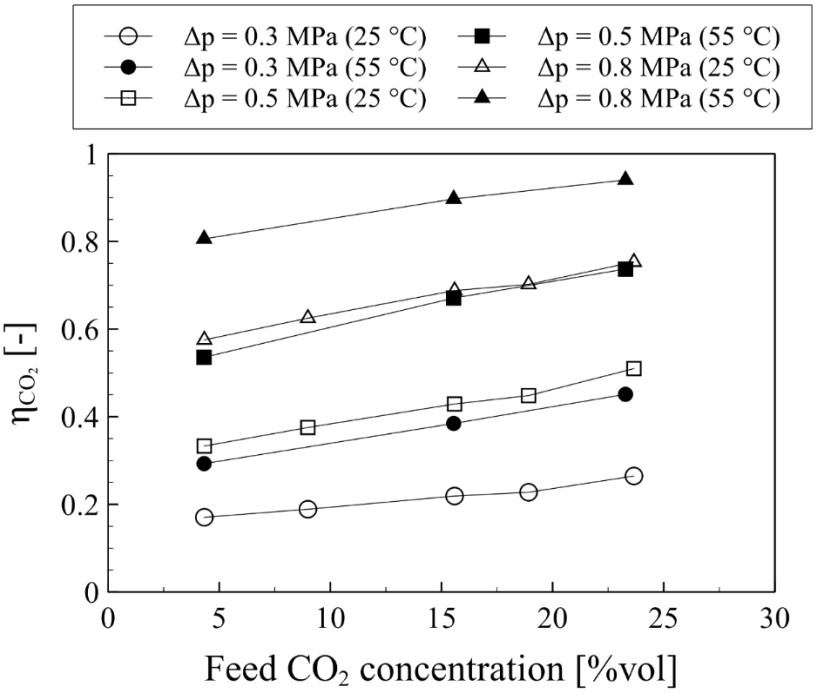

Figure 32. Recovery vs changing feed concentration for different temperatures. Higher process temperature showed improved CO_2 recovery.

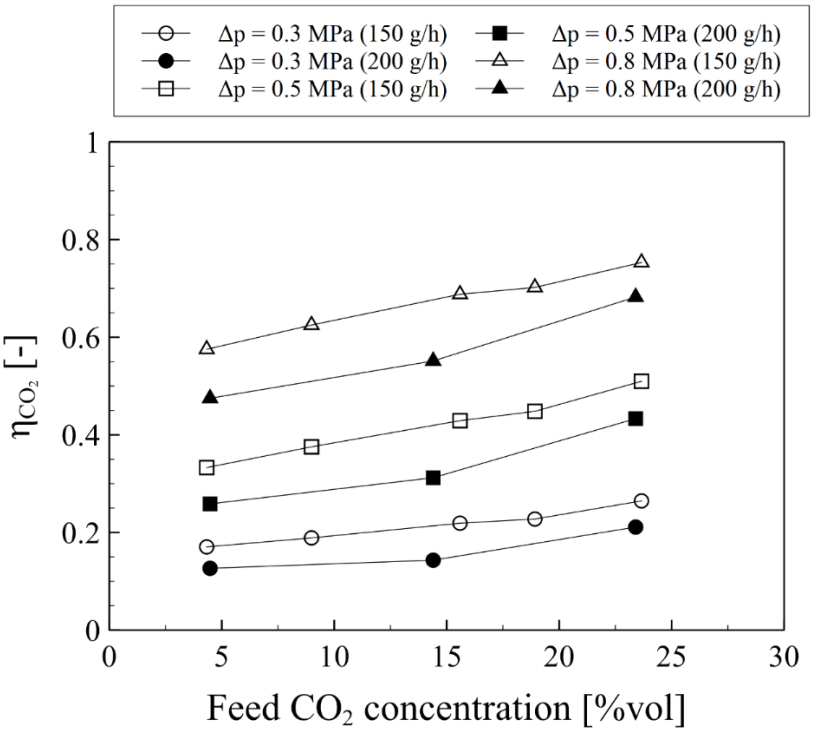

Figure 33. Effect of changing feed CO_2 concentration on recovery using different feed mass flowrates. Lower flowrates showed better recoveries.

4.3. Conclusion

The objectives of this work were two-fold: (1) a research focused on CO_2 membrane separation from flue gases and (2) experimental work on the membrane separation unit focused on defining the relationships between the separation performance and process parameters.

In the first part of this work, we initiated the reader into the problematic of CO_2 emissions, their impact, and the effort to reduce them – section 1. We identified the main industrial and process sources of CO_2 emissions and then briefly introduced the more traditional methods of CO_2 separation – section 2. Next, we made the case for CO_2 membrane separation and gas separation in general by listing the membrane separation advantages and disadvantages. Subsequently, we classified the membranes according to their materials and modules and introduced the principal membrane separation terminology – section 3.1 and 3.2. We then described mechanisms through which CO_2 can transported through various membrane types – section 3.3. Lastly, we focused on current and recent CO_2 membrane research and listed some important and relevant studies . By doing this research, we completed objective (1).

The experimental part started with characterizing the equipment end methods used in this work – section 4.1. For all experiments, the membrane unit RALEX GSU-LAB-200 was used. The experiments were designed around testing all possible process parameters: (a) variable CO_2 feed composition, (b) different temperatures, (c) different pressure drops, (e) varying inlet gas flows. The gas composition was based on typical flue gas compositions from literature shown in Table 1 and Table 2. CO_2 in feed varied from 5 to 25 %. This was one significant flaw of past research on membrane gas separation – not enough gas mixtures included and in case they were, mostly binary solutions were used. Therefore (a) was our prioritized variable. In following section - 4.1.3 – the experiment procedure was described and, subsequently, section 4.1.4 listed all the calculations done.

Afterwards, we presented our findings graphically in section 4.2. First, we showed the single-gas permeation tests and results. We showed that the single gas tests are necessary but should not be the sole available reference, as is the case many times in scientific papers. We stressed that variation in parameters such as temperature is important and has a big effect even on single gas separation (Figure 23). Later, we compared single gas and gas mixture permeances and showed that there is a big difference between the two - Figure 25 shows that CO_2 permeance dropped with increased pressure difference.

Finally, we presented the gas mixture (comprised of N_2+CO_2+O_2) experiments. The focus was on variable CO_2 concentration in feed and how it affects parameters such as permeance (Figure 26), CO_2 recovery (Figure 28) and separation factor (Figure 29). We showed that the permeance vs CO_2 concentration relation is quite nuanced. Both recovery and separation factor ramped up with increased CO_2 concentration. In Figure 30 we constructed a makeshift Robeson diagram (replaced ideal selectivity with separation factor) to summarize the membrane's performance.

In the end we showed that the permeance and recovery are affected by temperature/flowrate change (Figure 31, Figure 32, Figure 33). The analysis of achieved numbers left a lot to be desired, as the maximum permeances were in tens (around 40 GPU max.) while commercial membranes many times exceed a 1000 mark. Perhaps the one notable number is the recovery of >0.9 achieved at 55 °C, 0.8 MPa pressure difference and 24.5% CO_2 concentration.

Overall, membrane separation is an exciting branch of chemical engineering and one that has already found its way into industry so there is no question about its usefulness. There are challenges however, mainly in the field of research where many materials are being tried but few with industrial use. There also seems to be lack of variability in terms of tested gas mixtures and process parameters. But having said that, the huge leaps this technology has made in recent years is quite impressive and it will no doubt continue to find new uses.

5.References

1. Lacis, A. A. Greenhouse effect. https://www.accessscience.com/content/greenhouse-effect/299800 (2021) doi:10.1036/1097-8542.299800.
2. Friedrich, J. & Damassa, T. The History of Carbon Dioxide Emissions. https://www.wri.org/insights/history-carbon-dioxide-emissions (2014).
3. Core Writing Team, Pachauri, R. K. (ed. . & Meyer, L. A. (ed. . *Climate Change 2014: Synthesis Report. Contribution of Working Groups I, II and III to the Fifth Assessment Report of the Intergovernmental Panel on Climate Change*. (2014).
4. Nakao, S., Yogo, K., Goto, K., Kai, T. & Yamada, H. *Advanced CO2 Capture Technologies*. (Springer International Publishing, 2019). doi:10.1007/978-3-030-18858-0.
5. Balogh, J. M. & Jambor, A. Determinants of CO2 Emission: A Global Evidence. *Int. J. Energy Econ. Policy* (2017).
6. Fischedick, M. *et al. Climate Change 2014: Mitigation of Climate Change. Contribution of Working Group III to the Fifth Assessment Report of the Intergovernmental Panel on Climate Change*. (2014).
7. Zhou, W. *et al.* CO2 emissions and mitigation potential in China's ammonia industry. *Energy Policy* **38**, 3701–3709 (2010).
8. Benhelal, E., Zahedi, G., Shamsaei, E. & Bahadori, A. Global strategies and potentials to curb CO2 emissions in cement industry. *J. Clean. Prod.* **51**, 142–161 (2013).
9. Jawad, Z. A. *Membrane Technology for CO2 Sequestration and Separation*. *Membrane Technology for CO2 Sequestration and Separation* (CRC Press, 2019). doi:10.1201/b22409.
10. Xu, J. *et al.* Recent advances on the membrane processes for CO2 separation. *Chinese J. Chem. Eng.* **26**, 2280–2291 (2018).
11. Romero-García, A. G., Ramírez-Corona, N., Sánchez-Ramírez, E., Alcocer-García, H. & Segovia-Hernández, J. G. Effect of Flue Gas Composition on the Design of a CO2 Capture Plant. in 835–840 (2020). doi:10.1016/B978-0-12-823377-1.50140-3.
12. Powell, C. E. & Qiao, G. G. Polymeric CO2/N2 gas separation membranes for the capture

of carbon dioxide from power plant flue gases. *J. Memb. Sci.* **279**, 1–49 (2006).

13. Zhao, C. *et al.* Capturing CO2 in flue gas from fossil fuel-fired power plants using dry regenerable alkali metal-based sorbent. *Prog. Energy Combust. Sci.* **39**, 515–534 (2013).
14. Bosoaga, A., Masek, O. & Oakey, J. E. CO2 Capture Technologies for Cement Industry. *Energy Procedia* **1**, 133–140 (2009).
15. Ismail, A. F., Chandra Khulbe, K. & Matsuura, T. *Gas Separation Membranes*. (Springer International Publishing, 2015). doi:10.1007/978-3-319-01095-3.
16. Peter, J. *Membránová separace plynů a par*. (Deep Synergy, Prague, 2016).
17. Kagramanov, G. G. & Farnosova, E. N. Scientific and engineering principles of membrane gas separation systems development. *Theor. Found. Chem. Eng.* **51**, 38–44 (2017).
18. Basile, A., Iulianelli, A., Gallucci, F. & Morrone, P. Advanced membrane separation processes and technology for carbon dioxide (CO2) capture in power plants. in *Developments and Innovation in Carbon Dioxide (CO2) Capture and Storage Technology* 203–242 (Elsevier, 2010). doi:10.1533/9781845699574.2.203.
19. Mulder, M. *Basic Principles of Membrane Technology*. (Springer Netherlands, 1996). doi:10.1007/978-94-009-1766-8.
20. *Membrane Gas Separation*. (John Wiley & Sons, Ltd, 2010). doi:10.1002/9780470665626.
21. Barillas, M. K. *et al.* The CO2 permeability and mixed gas CO2/H2 selectivity of membranes composed of CO2-philic polymers. *J. Memb. Sci.* **372**, 29–39 (2011).
22. J, M. & M, F. CO2 Separation from Flue Gases Using Different Types of Membranes. *J. Membr. Sci. Technol.* **6**, (2016).
23. Torstensen, J. Ø., Helberg, R. M. L., Deng, L., Gregersen, Ø. W. & Syverud, K. PVA/nanocellulose nanocomposite membranes for CO2 separation from flue gas. *Int. J. Greenh. Gas Control* **81**, 93–102 (2019).
24. Liu, B., Tang, C., Li, X., Wang, B. & Zhou, R. High-performance SAPO-34 membranes for CO2 separations from simulated flue gas. *Microporous Mesoporous Mater.* **292**, 109712 (2020).
25. Koláčný, J. Membránová separace CO2 z emisních plynů. (Czech Technical University, 2020).
26. MemBrain s.r.o. Operační manuál: Laboratorní jednotka membránové separace směsi

plynů RALEX GSU-LAB-200. (2019).

27. MemBrain s.r.o. Technický list - Pilotní modul pro separac plynů P2.
28. Permentier, K., Vercammen, S., Soetaert, S. & Schellemans, C. Carbon dioxide poisoning: a literature review of an often forgotten cause of intoxication in the emergency department. *Int. J. Emerg. Med.* **10**, 14 (2017).